

**DESIGN OF A COMPUTER-CONTROLLED CURRENT
STIMULATOR FOR NERVE AND MUSCLE EXCITATION**

by

Mahmud Esad Arar

B.Sc., Mechatronics Engineering, Atılım University, 2009

Submitted to the Institute of Biomedical Engineering
in partial fulfillment of the requirements
for the degree of
Master of Science
in
Biomedical Engineering

Boğaziçi University

2015

ACKNOWLEDGMENTS

I would like to express my sincere gratitude and special thanks to my thesis advisors Prof. Dr. Mehmed Özkan and Assoc. Prof. Dr. Burak Güçlü for their endless tolerance, support and guidance throughout this work. I would like to specially thank to Dr. Güçlü for his assistance, recommendations, stimulating and sincere personality during the course of the thesis.

I am also grateful to Prof. Dr. Murat Gülsoy, Assist. Prof. Dr. Bora Garipcan and Assist. Prof. Dr. Evren Samur for their vital suggestions and for being a member of my thesis committee.

I would also thank to; The academic members of Engineering Faculty of Fatih Sultan Mehmet Vakıf University, in particular Prof. Dr. Fevzi Yılmaz, Prof. Dr. Burhanettin Can, Prof. Dr. Avni Morgül and Assist. Prof. Dr. Orhan Özhan for their advices and interests, All of the research assistants for their help and support, discussions and friendship attitudes.

I also would like to thank to İsmail Devecioğlu and Bige Vardar for their help and support, especially to Dr. Mustafa Zahid Yıldız.

Special thanks to all the other members of the Institute of Biomedical Engineering in terms of academic, administrative and personnel for the friendly and warm atmosphere I always found.

I also thank to Mechanical Engineer İbrahim Mutlu for his technical support.

Finally, I would like to thank my family for their endless support, encouragement and patience.

ABSTRACT

DESIGN OF A COMPUTER-CONTROLLED CURRENT STIMULATOR FOR NERVE AND MUSCLE EXCITATION

Electrical stimulation of excitable tissues has been widely used for diagnosing and treating neurological and muscular disorders. Electrical stimulation is also used to analyze and understand inherent functions of nerves and muscles. This study includes the circuit design of a current stimulator and its custom LabVIEW interface. The device is based on a modified Howland current-source topology due to its efficiency for injecting precise current without being affected by load resistance variations. Modified Howland current source converts voltage signals to desired current signals. The device is powered by an external power supply with high compliance $\pm 37 V_{dc}$. Waveforms are produced by using a computer audio output which is controlled by LabVIEW. Therefore any user can create its own user interface with any programming environment. Sinusoidal, square and triangle waveforms, in different frequencies, amplitudes and pulse widths, can be generated within the range of the sound card specifications. The device can generate both monopolar and bipolar current pulses with pulse duration of $0.05 - 10 ms$. Reliable frequency range of the system is $10 - 10,000 Hz$ and it can deliver $6.6 mA_{pp}$ at $10 k\Omega$ dummy load. This system can be easily constructed and is very inexpensive compared to commercial units. Both electrical and physiological tests are performed in order to prove that the device is running properly and it can be utilized in laboratory experiments of electrophysiology especially for somatosensory evoked potentials.

Keywords: Electrical stimulation, modified Howland current source, LabVIEW, audio output, electrophysiology.

ÖZET

SİNİR VE KAS UYARIMI İÇİN BİLGİSAYAR-KONTROLLÜ AKIM STİMÜLATÖRÜ TASARIMI

Canlı dokularının elektriksel olarak uyarılması, sinir ve kas bozukluklarının teşhis ve tedavisi amacıyla uzun yıllardır kullanılmaktadır. Ayrıca, elektriksel uyarım; sinir ve kasların doğasında olan işleyişini analiz etmek, kavramak ve anlamak için de yaygın olarak kullanılmaktadır. Bu çalışma bir akım kaynağı devresinin tasarlanması ve onun bilgisayar arayüzü ile kontrol edilmesini içermektedir. Cihaz tasarımında; değişken yük direncinden bağımsız olarak sabit akım verebilmesi için bu konuda yaygın olarak kullanılan gelişmiş Howland akım kaynağı topolojisi kullanılmıştır. Geliştirilmiş (Modified) Howland akım kaynağı uygulanan gerilimi istenen akıma çevirir. Cihaz, $\pm 37 V_{dc}$ besleme sağlayabilen harici bir güç kaynağı ile beslenmektedir. Dizüstü bilgisayar ses kartı LabVIEW tarafından sürülerek istenilen dalga şekilleri üretilmektedir. Sinüzoidal, kare ve üçgen dalga şekilleri, farklı genlik, frekans ve darbe genişliğinde ve ses kartının teknik özelliklerine ve sınırlarına uygun şekilde üretilmektedir. Cihaz monopolar ve bipolar darbe (puls) üretme özelliğine sahiptir. Cihazın darbe genişliği $0.05 - 10 ms$ arasındadır. Cihazın güvenli frekans aralığı $10 - 10,000 Hz$ olup, $10 k\Omega$ 'luk bir yük direncini $6.6 mA_{pp}$ akım ile sürebilmektedir. Bu cihaz kolaylıkla imal edilebilmesinin yanı sıra ticari ürünlere göre de daha ucuzdur. Cihaz elektriksel ve fizyolojik olarak test edilmiş ve çalıştığı kanıtlanmıştır. Laboratuvar ortamında elektrofizyoloji deneylerinde, özellikle de somatosensoriyel uyarılmış potansiyeller ölçülürken rahatlıkla kullanılabilir.

Anahtar Sözcükler: Elektriksel uyarım, geliştirilmiş Howland akım kaynağı, labVIEW, bilgisayar ses kartı çıkışı, elektrofizyoloji.

TABLE OF CONTENTS

ACKNOWLEDGMENTS	iii
ABSTRACT	iv
ÖZET	v
LIST OF FIGURES	viii
LIST OF TABLES	x
LIST OF SYMBOLS	xi
LIST OF ABBREVIATIONS	xii
1. INTRODUCTION	1
1.1 Motivation	1
1.2 Objectives	1
1.3 Thesis Outline	2
2. BACKGROUND	4
2.1 Bioelectricity	4
2.1.1 Nervous Tissue	4
2.1.2 Muscle Anatomy and Physiology	9
2.2 Electrical Nerve and Muscle Stimulation	14
2.2.1 Voltage to Current Converters	15
2.2.2 Stimulators from the Literature and Commercial Devices	15
2.2.3 Somatosensory Evoked Potential	17
3. MATERIALS AND METHODOLOGY	18
3.1 Stimulator Design Specifications and Voltage to Current Converter Topologies	18
3.1.1 Floating-Load Converters	20
3.1.2 Grounded-Load Converters	21
3.2 Stimulator Diagram and Analysis	25
3.2.1 Power Supply of the System	25
3.2.2 Isolation Amplifier and Current Source	27
3.2.3 Comparator for External Devices	34
3.3 Computer Interface and Software	38

3.4	Electrode Selection	41
4.	RESULTS	42
4.1	Calibration and Electrical Tests	42
4.2	Biological Experiments	45
5.	DISCUSSION	57
5.1	Limitations	57
5.1.1	Engineering Limitations	57
5.1.2	Biological Limitations	58
5.2	Comparison with Previous Stimulators	58
5.3	Suggestions for Improvement and Future Work	60
	APPENDIX A. Setup Photos	61
	REFERENCES	62

LIST OF FIGURES

Figure 1.1	Block diagram of the system	3
Figure 2.1	The structure of a neuron	5
Figure 2.2	Electrical and Chemical transmission	7
Figure 2.3	Chemical synaptic transmission	7
Figure 2.4	Action Potential	9
Figure 2.5	Conductance of voltage-gated ion channels	10
Figure 2.6	Structure of a muscle	10
Figure 2.7	Sarcomere structure	11
Figure 2.8	Muscle contraction	12
Figure 2.9	Neuromuscular Junction	13
Figure 2.10	Deep brain and Spinal cord stimulations	15
Figure 3.1	Floating Load Converters	21
Figure 3.2	Howland current source	22
Figure 3.3	Improved Howland current source	23
Figure 3.4	Adjustable Regulator	26
Figure 3.5	The power supplies	28
Figure 3.6	Main circuit scheme	29
Figure 3.7	RC Low-Pass Filter	29
Figure 3.8	Improved Howland Current Source	32
Figure 3.9	Comparator	34
Figure 3.10	Comparator circuit	36
Figure 3.11	Transfer curve	37
Figure 3.12	Interface of software 1	39
Figure 3.13	Block diagram of the software 1	39
Figure 3.14	Interface of software 2	40
Figure 3.15	Block diagram of the software 2	40
Figure 4.1	Sound card calibration	43
Figure 4.2	Stimulator calibration	44
Figure 4.3	Sound card frequency	45

Figure 4.4	Frequency response of the stimulator	46
Figure 4.5	Frequency response of the entire system	47
Figure 4.6	Loads vs. Current values	48
Figure 4.7	Loads vs. Current values 2	48
Figure 4.8	100 μs and 216 mV (yellow) and 1000 μs and 528 mV (blue) pulses are generated as the output of the sound card in order to trigger both the current stimulator and the comparator	49
Figure 4.9	1000 μs and 208 mV (yellow) and 1000 μs and 528 mV (blue) pulses are generated as the output of the sound card in order to trigger both the current stimulator and the comparator	49
Figure 4.10	Input signal is at 1000 Hz and 208 mV_{pp} where the output signal is at 1000 Hz and 20.8 mV_{pp} .	50
Figure 4.11	Sinusoidal input signal is at 100 Hz and 120 mV_{pp} where the output signal is at 100 Hz and 11.2 V_{pp} .	50
Figure 4.12	Square input signal is at 1000 Hz and 256 mV_{pp} where the output signal is at 1000 Hz and 23.2 V_{pp} .	51
Figure 4.13	Square waveform input signal is at 100 Hz and 136 mV_{pp} where the output signal is at 100 Hz and 11.2 V_{pp}	51
Figure 4.14	Averaged SEPs from rat under anesthesia after first injection, current of 2 mA at a pulse width of 100 μs and averaged at 100	54
Figure 4.15	Averaged SEPs from rat under anesthesia after second injection, current of 2 mA at pulse width of 100 μs and averaged is 400	55
Figure 4.16	Averaged SEPs from rat under anesthesia after second injection, current of 10 mA at pulse width of 250 μs and averaged is 370	56
Figure A.1	Entire setup 1	61
Figure A.2	Entire setup 2	61

LIST OF TABLES

Table 4.1	Comparison of Stimulation parameters of experiments Hayton et al. vs. Current Study.	46
Table 4.2	Latency values of previous study of Hayton et al. [14]. Current intensity is $1 - 2 \text{ mA}$ with 3s^{-1} frequency and 0.1 ms duration.	52
Table 4.3	Latency values of our physiological experiment.	52
Table 4.4	Amplitude values of previous study of Hayton et al. [14]. Current intensity is $1 - 2 \text{ mA}$ with 3s^{-1} frequency and 0.1 ms duration.	53
Table 4.5	Amplitude values of physiological experiment.	53

LIST OF SYMBOLS

Ω	Ohm, Unit of electrical resistance
F	Farad, Unit of capacitance
Hz	Hertz(cycles per second)
pp	Peak to peak (amplitude of a periodic variable)
I	Current
R	Resistance
V_{in}	Input voltage
V_d	Differential input Voltage
i_{out}	Output current
V_{dc}	Voltage of direct current
V_{sat}	Saturation voltage
$V_{threshold}$	Threshold voltage
V_{TH}	Threshold voltage high
V_{TL}	Threshold voltage low
V_{load}	Voltage on load
V_{ref}	Reference voltage
R_{out}	Converters output resistance
R_{load}	Load resistance
$R_{out\ max}$	Maximum load resistance driven by the device
R_{pullup}	Pull up resistor
$i_{out\ max}$	Desired maximum output current
$P1$	Positive peak 1
$N1$	Negative peak 1
k	Kilo (10^3)
m	Milli (10^{-3})
μ	Micro (10^{-6})
n	Nano (10^{-9})

LIST OF ABBREVIATIONS

A	Ampere
V	Volts
AC	Alternating current
DC	Direct current
SEP	Somatosensory evoked Potential
MRI	Magnetic Resonance Imaging
EIT	Electrical impedance tomography
IC	Integrated Circuit
TTL	Transistor-transistor logic
ATP	Adenozin triphosphate
EEG	Electroencephalography
EP	Evoked potential
CNS	Central nervous system
BJT	Bipolar junction transistor
MOSFET	Metal oxide field effect transistor
MS	Multiple sclerosis
V-I Converter	Voltage to current converter
FES	Functionoal electrical stimulation
FNS	Functional neuromuscular stimulation
EMG	Electromyography

1. INTRODUCTION

1.1 Motivation

In late 17th century, Luigi Aloisio Galvani and his assistant defined 'bioelectricity' in their experiment on frogs [1]. During the early days of bioelectricity, electrical current is applied to humans for treatment of pain . Later, it started to be used for diagnosis, monitor and treatment of diseases (i.e. primo vascular diseases). Most recently, functions of some organs can be restored or supported by using bioelectricity devices. For example, arms of a motor-disabled person can be moved by electrical stimulation of muscles [2].

Electrical stimulation of excitable tissues, such as nerve and muscle, has been a fundamental experimental tool in teaching life sciences and also in biomedical research. In order to excite a tissue, electrical stimulators (i.e. constant current supplies) are used. The commercially available stimulators are extremely expensive and some might not be controllable by the hardware (i.e. audio output) of personal computers available in laboratories [3]. In addition, requirement for additional extension (e.g. external isolation unit) on stimulator device increase the cost. Furthermore, these devices may require periodic maintenance and calibration or repair only by the supplier which means dependence on the supplier and an increase in the cost.

1.2 Objectives

The objective of this masters thesis is to design a current stimulator from off-the-shelf components with a simple design that satisfies the needs for biomedical applications. The design has high compliance and high output resistance, and is able to supply high current levels. The thesis also includes design of a stimulator control-software that can be easily modified for needs.

The design presented in this study is based on improved Howland current source topology which has very high output impedance when resistors are well-matched according to Eq. 3.13. An integrated circuit (IC) ISO 124 is used for isolation. The device has a very high compliance (closer to $\pm 40 V_{dc}$ but the saturation of IC's allow $\pm 33 V_{dc}$ at the output stage however our power supply is about $\pm 37 V_{dc}$). A power op-amp with high supply voltages had been chosen. This IC is OPA 453 and it is able to give $50 mA$ and it can also reach $125 mA$ in extreme conditions. The aimed and planned output current is somewhat greater than $100 \mu A$ and can reach even $10 mA_{pp}$ where the load resistances are lower than $6.6 k\Omega$ where the tissue resistance of experimental subjects does not even reach 100Ω due to application was subdermal in the current tests. Frequency range considered here was $10 - 10,000 Hz$ and it already meets the requirements for SEPs. The duration of pulse was varied between $0.05 - 10 ms$, but sound card can supply until $100 ms$ range. The final device had a high compliance of $\pm 37 V_{dc}$ and could supply $6.6 mA_{pp}$ current levels for $10 k\Omega$ dummy-load or $66 mA_{pp}$ current level for $1 k\Omega$ dummy-load. However, tissue damaged may occur in subdermal applications at this level. In addition, op-amp should be protected and cooled very well. The device could generate pulses with duration between $50 \mu s$ and $100 ms$. Flow diagram of the study is presented at (Figure 1.1).

1.3 Thesis Outline

This thesis consists of 5 chapters: In chapter 2, anatomical and physiological information about nerves and muscles are given. This chapter also includes the background information about topology and design of electrical stimulators. Chapter 3 includes the information about the hardware and software of the entire system. Attempted circuit topologies, the final design topology and the design steps are presented in detail. Chapter 4 gives the experimental results of the device. Two experiments were performed; the first one is the electrical evaluation of the circuits. The second experiment is the test of the final device on rat nervous system. Chapter 5 gives the discussion on the final device; limitations and suggestions are mentioned.

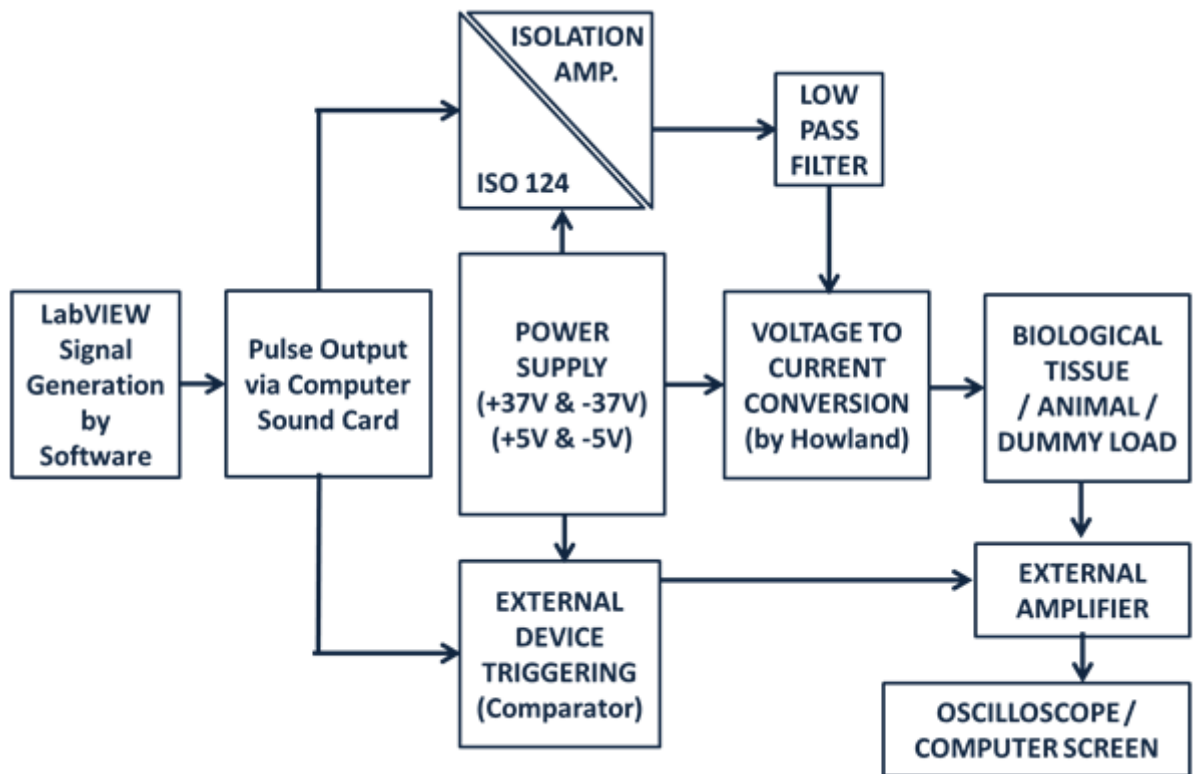


Figure 1.1 Block diagram of the system is designed for electrophysiological experiments.

2. BACKGROUND

2.1 Bioelectricity

Nerve cells and muscles are the two primary types of excitable tissues in living beings. Nervous tissue is composed of nerve cells and glial cells. Nerve cells receive and transmit nerve impulses whereas glial cells support and nourish them by providing the necessary nutrients to the neuron. Muscles tissues enable muscles' ability to contract in response to stimulus.

2.1.1 Nervous Tissue

Nervous system is composed of two main classes of cells that are nerve cells or neuron and glial cells or glia. Nervous system rapidly communicates other system. This ability can be provided by neurons features that are; Asymmetry of their morphology and electrical-chemical excitability.

- **Structure of a nerve cell**

A nerve cell is consisting of four parts; the cell body (soma), dendrites, axon, and presynaptic terminals (Figure 2.1). These parts play important role in the process of signal generation and communication with other neurons. The soma (body) is the place of the metabolic activities required for maintenance of neuron. Dendrites receive signals from other neurons while axons transmit the received signals to adjacent neurons. Electrical signals are carried for long distances through the axons. The nerve impulses are known as action potential and initiated at the soma. An action potential has amplitude of 100mV which does not change (due to regeneration of action potentials

on the axons in frequent intervals) throughout the axon [4, 5].

Conduction speed of the action potential depends on diameter of the axon. Larger diameter leads to larger conduction speed. Axons are surrounded by myelin sheaths made of lipid (fat) and protein which insulates the axons. There are gaps between myelin sheaths wrapping the axon called nodes of Ranvier at which the axons are not insulated thus generation of electrical activity.

Synapse is the special structure where the neurons communicate to each other via electrical or chemical signal. Presynaptic and postsynaptic neurons are separated by a special gap called synaptic cleft.

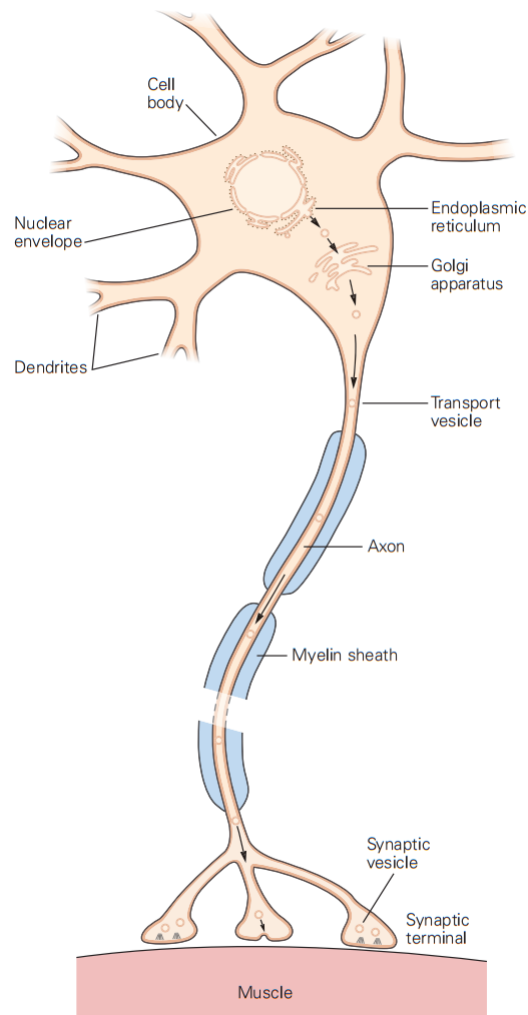


Figure 2.1 The structure of a neuron [5].

- **Synaptic transmission**

Synaptic transmission is the process of how neurons communicate each other. Synaptic transmission is accomplished by two ways; electrical or chemical. Electrical transmission is direct transfer of depolarization across membrane of presynaptic neuron to post synaptic neuron through gap junctions which is the small hole in the cell's membrane. Chemical transmission is through chemicals called neurotransmitters released into the synaptic cleft which binds to receptor located on the post synaptic neuron and change its electric potential. Moreover, a neuronal signal from presynaptic terminal to post synaptic terminal can be amplified at chemical synapse so if it is a small signal it can be converted to a large signal at postsynaptic terminal. Synaptic transmission can be between nerve-to-nerve, nerve-to-muscle and muscle-to-muscle.

Electrical transmission generates current, by the action potential at the presynaptic terminal, directly towards to postsynaptic cell. In contrast, chemical transmission generates current at the postsynaptic terminal by action potential forcing the vesicles of presynaptic terminal releasing chemical substances called neurotransmitters.

Electrical synapses and chemical synapses are different then each other in terms of structure. In electrical transmission the gap between the presynaptic and postsynaptic terminals is smaller compared to chemical transmission. The gap-junction channels, in electrical transmission, provide communication of between presynaptic and postsynaptic neuron. Outgoing currents leave positive charges inside the presynaptic cell membrane which cause a depolarization of the cell whereas incoming currents via the gap-junction channels carry positive charges inside the membrane causes a depolarization at the cell. If the depolarization reaches the threshold value, postsynaptic cell's voltage-gated ion channels suddenly open and create an action potential. On the contrary, in chemical transmission neurotransmitters released to synaptic cleft bind to the receptors located on postsynaptic cells (Figure 2.2).

To get larger currents at postsynaptic cells, presynaptic cell should be bigger than usual due to having many ion channels on its membrane. In contrast, postsynaptic cell should be smaller than usual in order to increase the input resistance. When the input resistance is obtained small, the Ohm's law is applied $V = IR$. Currents flowing from presynaptic to postsynaptic cell causes a large voltage change when the

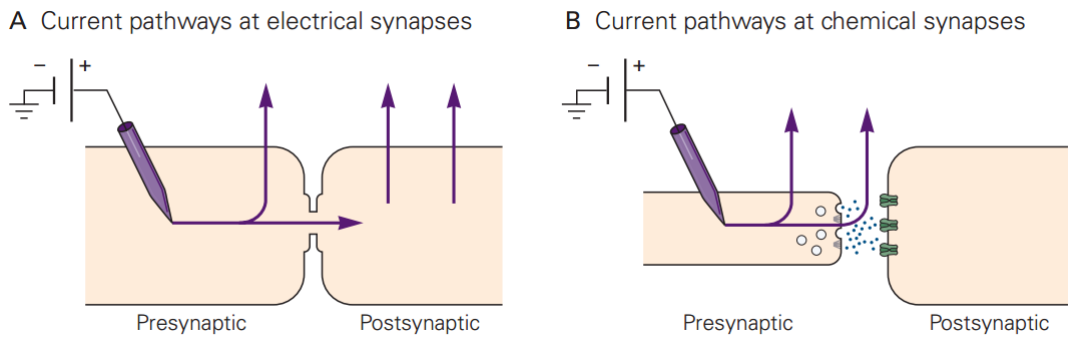


Figure 2.2 Electrical transmission (left), Chemical transmission (right) [5].

resistance of the presynaptic cell is small.

Presynaptic action potentials cause depolarization, at the postsynaptic cells, for generating action potentials. In electrical transmission, weak currents of presynaptic cell can depolarize the postsynaptic cells. In contrast, threshold value must exceed in the presynaptic cells in order to generate an action potential to make neurotransmitters released to trigger postsynaptic cells in the chemical transmission (Figure 2.3). Electrical synapses can be both depolarizing and hyperpolarizing [4]-[6].

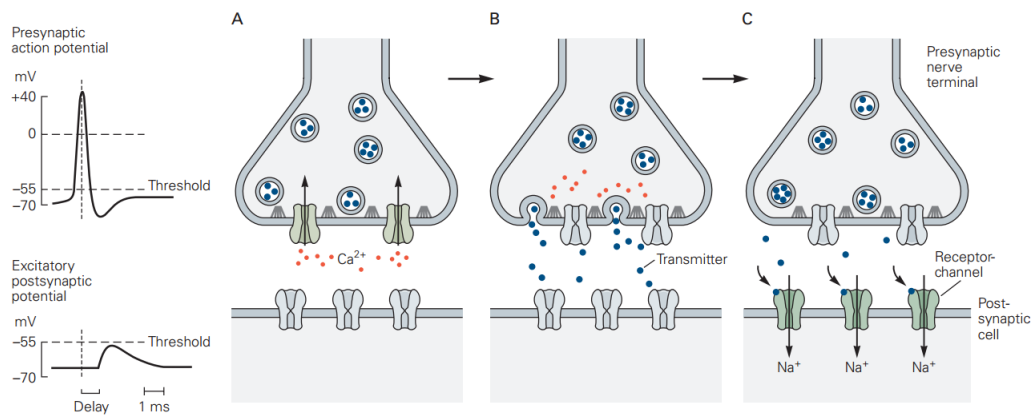


Figure 2.3 Chemical synaptic transmission [5].

• Action potential generation

Neurons are employed for generating electrical signals to carry neural information. Process of the generation of electrical signals depends on the amount of ions that flowing through the neurons' plasma membranes. Neurons are at resting potentials means a relatively stable membrane potential in which state the ion channels are

closed and there is no inward or outward ion flow. The resting membrane potential is about $-70mV$. In contrast, when a dynamic voltage change occurs, neurons generate an action potential where the transmembrane potential is positive. An action potential is generated at the soma and moves through axon of the presynaptic neuron. Myelin sheaths wrapping the axon both insulate and increase the speed of conduction [4]-[7].

Voltage-gated ion channels play an essential role for generating action potentials and also these channels are responsible for electrical excitability of neurons. Action potentials have four important features which are; they have a threshold value, they are all-or-none events, the amplitude of an action potential does not change along the axon (regeneration at the nodes of Ranvier), and they are followed by a refractory period in which the voltage-gated ion channels require time to recover from inactivation.

Action potentials have a threshold value around $-55mV$ which should be reached to generate an action potential. The amplitude of an action potential does not depend on the amount of the current though the frequency of the amplitude is dependent on the intensity of a stimulus. This is so called 'all-or-none event' of the action potentials. Amplitude of an action potentials are constant during propagation along the axon.

Figure 2.4 shows a plot of a typical action potential with several phases from the beginning of a voltage change across the cell membrane.

When the membrane potential reaches a threshold value, voltage-gated Na^+ channels open and depolarization occurs when the channels open. Depolarization increases the conductance of Na^+ ions and Na^+ ions flows through the channels into the cell which leads to dynamic increase in the membrane potential. Increase in the membrane channel cause more channel to open until all the ion channels open. When the ion channels are inactivated due to rapid influx of sodium ions, electrochemical gradient returns to resting membrane potential (repolarization).

Refractory period is the time interval when the cell cannot be stimulated by any of the stimulation method because when Na^+ channels are induced once and cannot be excited again before recovery. Refractory period lasts when the relevant cell reaches the resting potential. High concentration of Ca^{2+} at the exterior of the cell increases the threshold positively and stimulation becomes more difficult. In contrast, low level of Ca^{2+} causes muscle spasm. In order to reach the threshold value of the tissues immediately, stimulus strength and duration is important (Figure 2.5) [5, 7, 8].

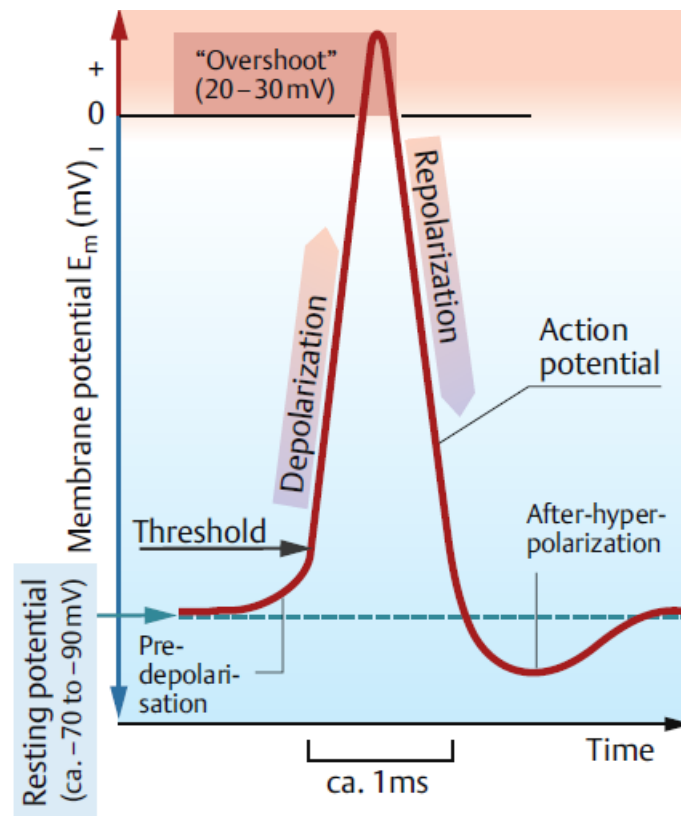


Figure 2.4 Action Potential [8].

2.1.2 Muscle Anatomy and Physiology

Muscles are responsible for many essential tasks of motility of living beings. The ability of locomotion also can be provided just by systems includes muscles. They provide movement by shortening and turning to original state.

- **Structure of muscle**

Muscle cells or fibers (myocytes) consist of hundreds of myofibrils which are covered by sarcoplasm. Myofibrils are the smallest unit in muscle systems and with sarcoplasm they are contractile element of the muscles. Sarcolemma is the cell membrane which encases the sarcoplasm, nuclei, other energy and oxygen supply units. Myocytes, created by the hundreds of myofibrils and sarcoplasm, creates the muscle fibers which are covered by endomysium. Muscle fibers build up the bundle of fibers

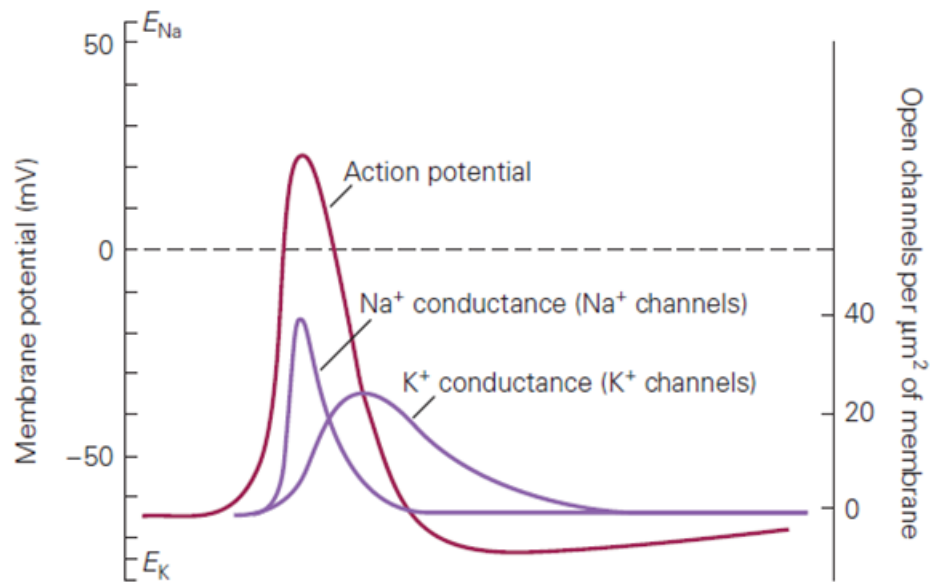


Figure 2.5 Conductance of voltage-gated ion channels [5].

that are surrounded by perimysium. Finally whole muscle is surrounded by epimysium (Figure 2.6).

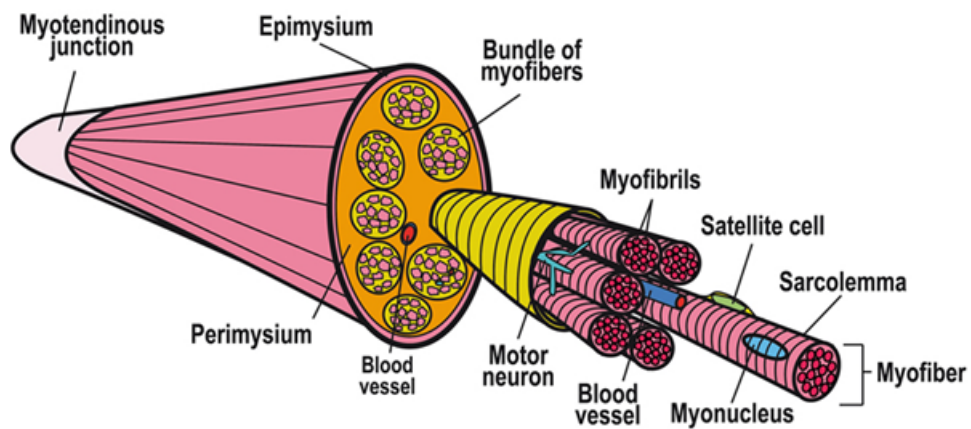


Figure 2.6 Structure of a muscle [9].

Myofibrils are made up of protein myofilaments that are actin, myosin, tropomyosin and troponin filaments. Z-plates divide the sarcomeres, which is the smallest unit of fiber, are the contractile elements of fiber (Figure 2.7). Z-plates consists actin filaments about 2000 which align just middle of the Z-plates. I-band occurs here where the actin filaments are aligned on Z-plates. A-bands place a point where actin and myosin filaments coincide in the middle of the sarcomere. H-zone placed just middle of the sarcomere. M-disk (plate) is placed just middle of the myosin filament [6, 8].

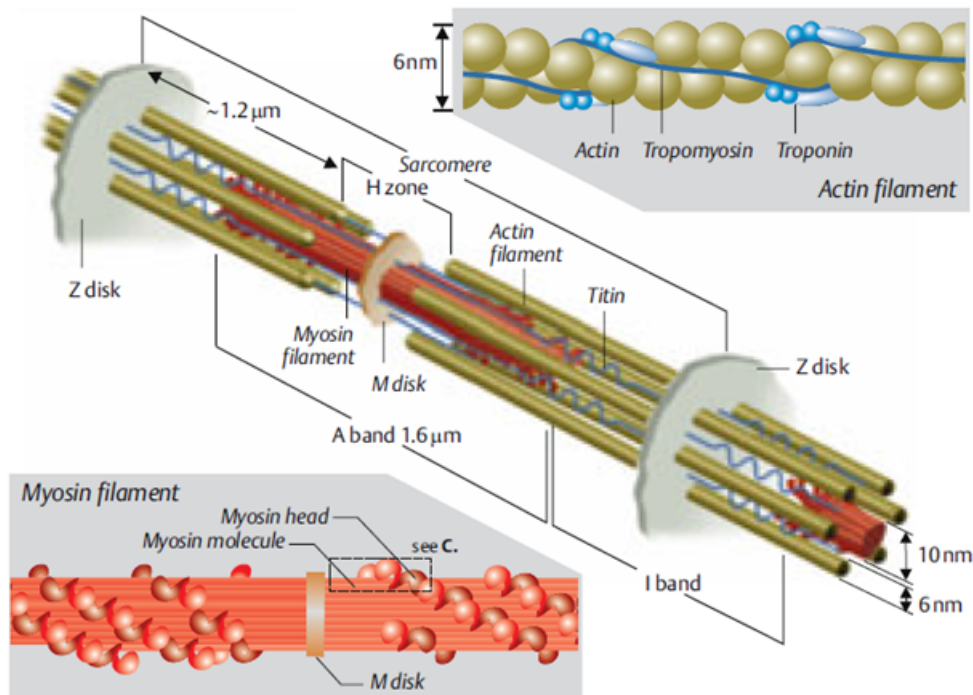


Figure 2.7 Sarcomere structure [8].

• Muscle contraction and Neuromuscular junction transmission

An action potential should be gathered to achieve a stimulation of a muscle fiber. Voltage-gated Na^+ channels, in the sarcolemma, are activated by a current which is generated when the acetylcholine is released at the motor end plate. This excitation is converted to a contraction called electromechanical coupling. Sarcolemma's dihydropyridine receptors are voltage sensors of muscle cells for searching depolarization so when these receptors are excited the process of excitation and contraction is activated [8].

Muscle contraction occurs when the myosin molecules bind to actin and pull the actin to the center of sarcolemma. This binding form is named as cross-bridges that are a special shape of binding where the myosin head binds to actin with an angle. This pulling action is called as sliding filament mechanism which is done by ATP energy and end with muscle contractions by shortening. Contraction of the muscle causes a decrease of length between the muscle and its attachments then they become close to each other (Figure 2.8). The energy which muscle needs for contraction is provided by myosin by hydrolyzing ATP to ADP [4].

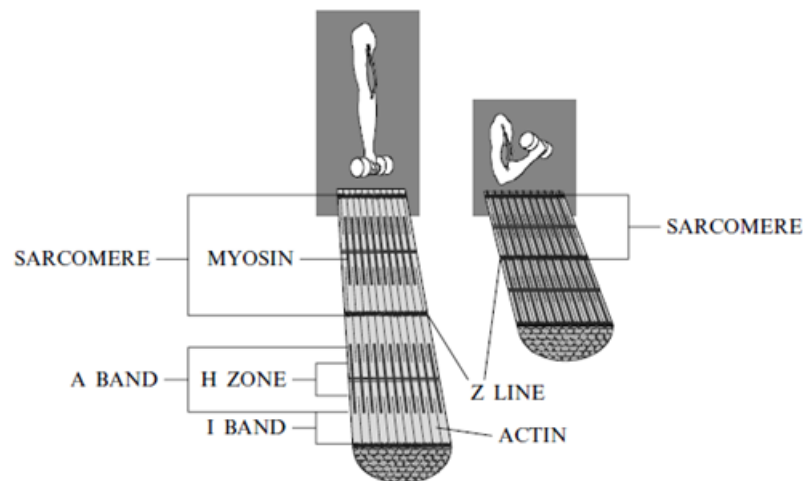


Figure 2.8 Muscle contraction (Isotonic) [4].

Muscles fibers and nerves are getting connected to each other at neuromuscular junction. The communication between the muscles and nerves is as follow: Sensory receptors of the muscle systems gather the sensory information and convey it to brain via spinal cord then motor nerve endings transmit the task to muscle via same path and then muscle contracts in order to perform the task send by motor cortex. Motor axons of the nerves can split up into many branches and make connections to muscle cells in order to supply and stimulate.

A synapse between a muscle and a nerve is named: the neuromuscular junction (Figure 2.9). This gap fills by acetylcholine, a neurotransmitter releases from the vesicles of axon, which binds to motor end plate of the sarcolemma. It results opening of the Na^+ channels in the sarcolemma so action potential of a muscle fiber is achieved. Action potential expands along the sarcolemma and reaches T tubules (transverse tubules) where the Ca^{2+} is released.

Ca^{2+} release causes cross-bridges of myosin which produce contraction of muscle. Contraction process is terminated when acetylcholinesterase hydrolyzed acetylcholine so sarcolemma permeability of Na^+ is decreased. So the muscle relaxes and turns its original state. Relaxation process is obtained by Ca^{2+} is no longer available in the process because ATP is consumed to remove Ca^{2+} and active sites are disappeared so actin and myosin cannot converge and finally muscle turns to its original state.

Two types of skeletal muscle fibers are available. These are fast and slow fibers. Fast fibers are powerful and contain lots of myofibrils. Fast types contracts strongly

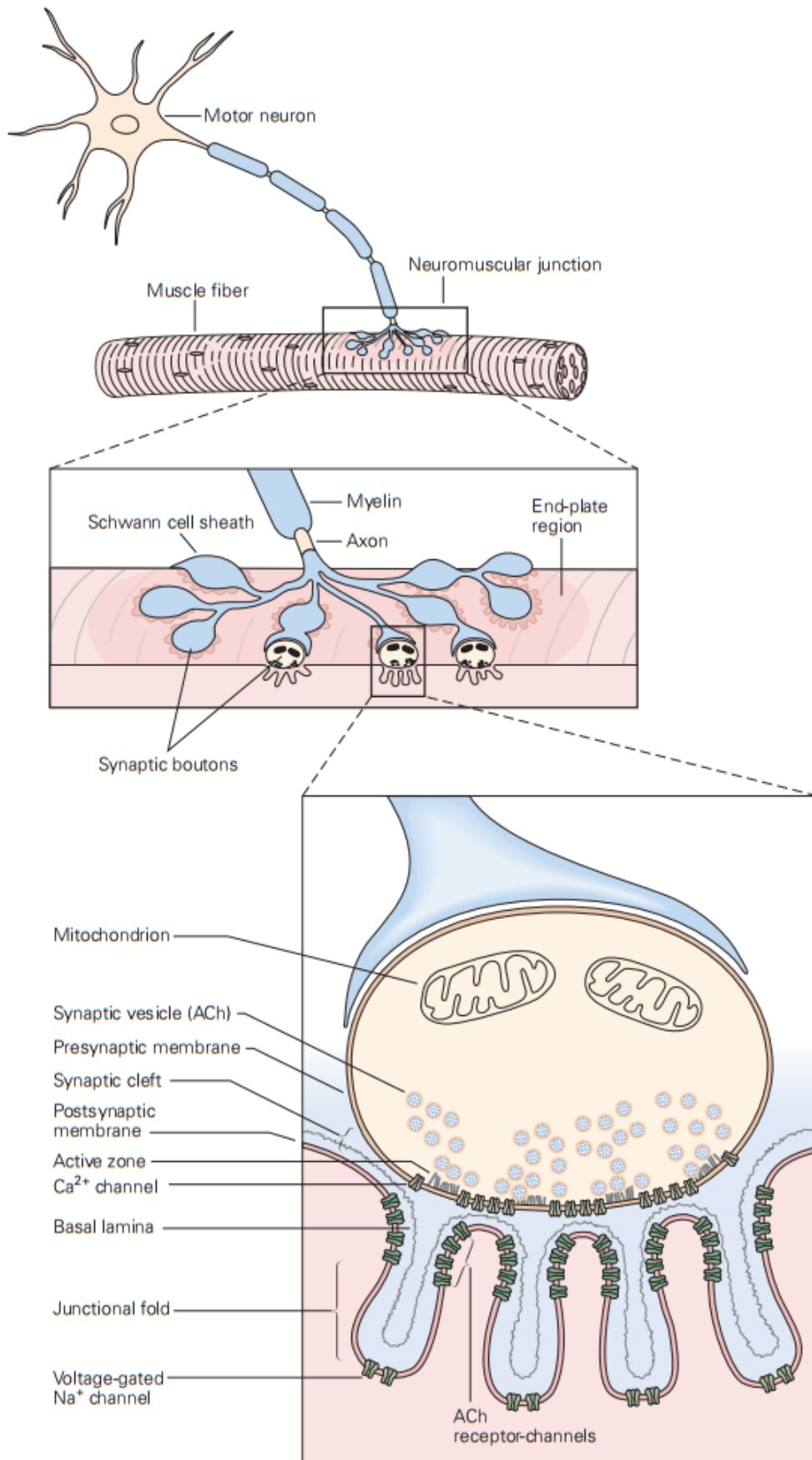


Figure 2.9 Neuromuscular Junction [5].

use ATP and reaches fatigue (muscle is not available for activation) immediately. Most of the skeletal muscles are made up of fast fiber. Fast fibers need more storage of glycogen (needed for production of ATP) for more ATP supplement. Slow fibers can produce low forces but they have high endurance limit.

2.2 Electrical Nerve and Muscle Stimulation

Electrical stimulation of the nerves and muscles is an artificial exciting method in order to understand the bioelectrical nature of these tissues. This technique is used in diagnostic and therapeutic medical applications. Furthermore, electrical stimulators have been widely used in biomedical training and research. The basis of electrical stimulation is the excitation of a cell by applying current from a constant current source. The current changes the electrical potential on the membrane of the cell and a response (e.g. action potential or muscle contraction) occurs if the threshold is reached [6].

In examination nervous system, electrical stimulation is applied on the periphery (i.e. skin surface) to excite peripheral nerve endings and to elicit event related potentials (EP) on brain surface. These potentials are recorded with EEG techniques and characteristic of the recorded signal (e.g. timings of potential peaks) is analyzed. Similarly, for recovery or regulation of an organ's function, electrical stimulation is applied on the organ with different techniques and stimulation parameters depending on the bioelectrical and functional properties of the organ. For example, by stimulating peripheral muscles or nerve fibers innervating these muscles on a motor-disabled person, it is possible to move specific limbs and regain the control of that limb to the subject in combination with brain-machine interfaces [2, 10]. In order to cope with pain, some therapeutic stimulation devices are implanted into the living bodies [2]. These devices have no significant side effects. Two examples are shown in Figure 2.10 presenting the deep brain stimulation (on the left) and spinal cord stimulations (on the right) for pain relief [2]. Electrical stimulation of central nervous system (CNS) is also used for the treatment of epileptic seizures and obsessive compulsive disorders [2].

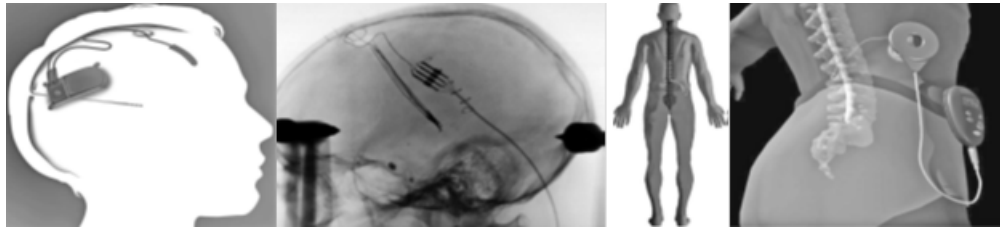


Figure 2.10 Deep brain (left two) - Spinal cord (right two) stimulations for pain management [2].

2.2.1 Voltage to Current Converters

Voltage to current converters (V-I converters) are the most preferred topology for electrical stimulator devices. These devices convert a constant voltage given to their input into a constant current level independent of the load. The V-I converters can be constructed using different electronic circuit topologies and components. BJT, MOSFET, and Op-amp applications are widespread. Op amp based circuits become prominent due to the easiness of the design; just a few additional components are required to set the characteristic parameters of the circuit (e.g. the gain) [11]-[12].

2.2.2 Stimulators from the Literature and Commercial Devices

Stimulators are the devices that are used to excite nerves and muscles. Stimulators can generate continuous signals or repeating pulses whose amplitude, duration and pulse width can be adjustable. The flexibility is an important parameter for stimulators. These devices are used in many areas of medicine and biomedical research. Some of researchers, in different areas of life sciences, use these devices in their research areas. Device parameters can be different depending on the research or usage area and also the experimental subjects (i.e. human, rat, monkey). Commercial stimulators usually meet the needs of studies but they are very expensive. On the other hand, custom-made stimulators are both inexpensive and flexible in use.

Stimulators are commonly designed in order to meet the requirements of the studies. For example, in the study of cortical microstimulation, Romo et al. injected currents between $40 - 100 \mu A$ while the frequency was about 12 Hz and the duration

of each phase of electrical pulse was 0.2 ms [13].

On the other hand, study of Hayton et al. electrically stimulated peripheral nerves to see the anesthetic agent's relation with latencies and amplitudes of somatosensory evoked potentials. They used $1 - 10\text{ mA}$ current levels with duration of 0.1 ms delivered at 3 Hz [14].

Another study is about stimulator design for transcutaneous stimulation by McPartland et al. [15]. They designed a device which can supply currents up to 100 mA with a frequency range of $10 - 60\text{ Hz}$ and a pulse width of 1 ms .

Final, in the study of Tucker et al., they build a current stimulator for electrical impedance tomography (EIT). The device had a frequency range of $1\text{ kHz} - 1\text{ MHz}$ and could supply current levels up to 2 mA [12].

Some of the commercial stimulators can have a very wide range of stimulation parameters, but their prices are very high to have them in the laboratories for students experiments; for example, Model DS7A of Digitimeter, 6002 Basic Stimulator of Harvard apparatus ($\$1,400$), SD9 Square-Pulse stimulator of Grass Technologies ($\$1,700$), BSL Stimulator of BIOPAC systems ($\$3,600$), Model 2100 Isolated pulse stimulator of A-M system ($\$1,800$) and DS8000 of World Precision Instruments ($\$6,000$).

Commercial devices have distinct parameters; i.e. BIOPAC STMISOLA linear isolated stimulator has two output stages for high current mode (100 mA) and low current mode (10 mA) with compliance of $\pm 200\text{ V}$, $\pm 10\text{ V}$ control voltage and maximum sine frequency of 30 kHz . It is well suited for transcranial direct current stimulation. On the other hand, Digitimeter-DS2A/DS3 stimulators are constant current/voltage isolated stimulators. DS3 provides; $32\mu\text{A}$, $320\mu\text{A}$, 3.2 mA and 32 mA maximum currents at 4 stages. Pulse width is from $10\text{ }\mu\text{s}$ to 100 ms with $\pm 10\%$ accuracy.

Güçlü [3] designed an isolated, low-cost constant current source for laboratory experiments. This stimulator supply 1.5 mA maximum current with $\pm 15\text{ V}$ compliance and its linearity is perfect in the range of $1 - 200\text{ }\mu\text{A}$ and frequency range is about $20 - 5000\text{ Hz}$.

Jaw et al. [16] designed a programmable stimulator appropriate for many neuroscience experiments. The device has programmable ranges of pulse duration ($5\mu\text{s}$ to 65 ms) and frequency (can be $< 0.0005\text{ Hz}$). In addition, the current output range of the device is between $0 - 10\text{ mA}$. It has an isolation unit to minimize stimulus

artifact.

In order to design a specific or a general purpose electrical stimulator, the needs should be defined first. Stimulators used in neurostimulation, need high compliance constant-current and isolated output [17].

2.2.3 Somatosensory Evoked Potential

Somatosensory evoked potentials (SEPs) are electrical responses of nervous system to sensory nerve stimulation. After peripheral nerve fibers are activated, this sensory information reaches to the somatosensory cortex causing a compound electrical potential (due to many active cortical neurons) on the brain surface. SEPs are generally used for diagnosis and monitor of some nervous system disorders, such as Multiple sclerosis, Transverse myelitis, Spinal cord injury. SEPs are unique choices when MRI is not sufficient to monitor dysfunction or abnormalities of the afferent nerves. SEPs are also used in spinal cord operations widely, in order to observe if any damage occurs on the sensory pathway.

Stimulation is performed by electrical excitation of the nerve endings in the skin. Mechanical activation is rarely used. However, use of electrical excitation is more popular and also preferred method of activation.

Stimulus intensity is arranged according to the electrode type and stimulation site and depth. **Stimulus can be constant voltage, but the current level may alter too much (causing injuries) depending on the variations of tissue impedance and electrode-tissue interface. Constant current stimulation gives more proper results compared to voltage stimulation.** Constant current is more sustainable for the stimulation since although tissue impedance changes, a constant level of current flows through nerve fibers. Pulse duration of the electrical stimulus is about 0.2 *ms* [18].

3. MATERIALS AND METHODOLOGY

This chapter of document consists how the electrical stimulator is designed, tested and constructed. Main topics of the chapter are stimulator design specifications, stimulator diagrams and analyses, computer interface-software and electrode selection.

The device or the system has been mentioned as electrical stimulator or just a stimulator, in this thesis, includes many subsystems such as; a power supply: for supplying energy needed by whole system, a voltage to current converter (V-I converter): for acquiring constant current, a comparator: for triggering an external amplifier, and a computer as the controller: for driving entire system.

3.1 Stimulator Design Specifications and Voltage to Current Converter Topologies

The electrical stimulator of this study is designed in accordance with laboratory employment in order to perform electrophysiology experiment which is one of the basic needs of biomedical laboratory education. General requirements for an electrical stimulator, used in electrophysiology experiments, vary in terms of purpose of usage. A constant current source should supply desired currents as desired amplitudes, frequencies, repetition times, and pulse-widths according to in which application will it be employed. Electrical stimulation can be implemented as direct or alternating current types, in a various waveform shapes as monophasic or biphasic square waves. The amplitude differs according to the place where electrical stimulation is applied intradermal (dermis layer), subcutaneous (subcutaneous tissue), or transcutaneous.

The stimulators output impedance must be high enough to supply constant current that is not affected by various resistances. Current sources also requires high output impedance so current sources are preferred, instead of voltage sources, in order to electrically excite the living tissues. In this study a V-I converter topology has been decided to be used for getting constant current which can be controlled by variable

voltage. Constant current stimulation is more effective than constant voltage stimulation in electrophysiology so constant current stimulators are much more preferable than any others.

Positive-negative, biphasic pulses or pulse trains can be produced as desired waveforms by software. Input and output waveforms of this study are characteristically positive square-pulses where its amplitude, pulse-width, pulse repetition are controlled by software. Continuous sinusoidal, square and triangular waveforms are also generated by software in order to electrically evaluate the system specifications.

Voltage to current converters which are also called as transconductance amplifiers, convert an applied input voltage to an output current that is amplified being multiplied by transconductance gain. $i_{out} = Av_{in}$, is the formulation of the transconductance amplifier, where i_{out} is the output current that is amplified by means of A and v_{in} is the input voltage. Equation 3.1 is the more realistic expression of a V-I converter characteristic.

$$i_{out} = Av_{in} - \frac{1}{R_{out}}v_{load} \quad (3.1)$$

$$v_{load} = i_{out}R_{load} \quad (3.2)$$

In equations (3.1 and 3.2), v_{load} is the resulting voltage when i_{out} flows over the load resistance (R_{load}). R_{out} is the converter's output resistance which is encountered by the load. For more stable i_{out} , a perfect V-I conversion is needed so, i_{out} must be totally independent of v_{load} it means that i_{out} should not varies with R_{load} , therefore, we have $R_{out} = \infty$. R_{out} can be infinite, in theory. However, in practice R_{out} can just approach high resistance values but not be infinite. This fact determines the quality of conversion and also the stability of i_{out} [11].

An output load, should be committed to the output port of converter, is crucial in order not to cause any malfunction of circuit due to current flow problems. The

voltage compliance shows the maximum values of v_{load} before saturation takes place.

V-I converters are divided into two groups; Floating-Load converters and Grounded-Load converter. In floating-load converters, load is not committed to ground and be used as a feedback component on the other hand, grounded-load converters have a load component one of whose terminal is grounded.

3.1.1 Floating-Load Converters

Floating-load converter means load is used as a feedback component in the circuit. Two kinds of floating type converters exist. These are non-inverting (Figure 3.1(a)) and inverting types (Figure 3.1(b)). Sensitivity resistance (R) which decides current (i_{out}) in accordance with input voltage (v_{in}) and i_{out} flows from output terminal to inverting input terminal of the op amp and gives the equation of $v_{in} = i_{out}R$ then eq. 3.3 is found. The advantages of non-inverting type are; source sees an infinite resistance at the input of the op amp and op amp drives the load by itself. The drawback of non-inverting type is; the limited voltage compliance $[(v_{OL} - v_{in}) < v_{load} < (v_{OH} - v_{in})]$.

$$i_{out} = \frac{1}{R}v_{in} \quad (3.3)$$

In any types of load, op amp's output carries the current i_{out} which is dependent on input voltage (v_{in}) and sensitivity resistance (R) and independent from voltage on the load (v_{load}). In non-inverting type, op amp keeps its output voltage at $v_{out} = v_{in} + v_{load}$ in order to keep i_{out} stable.

On the other hand, inverting type floating load converter (Figure 3.1(b)) draws a current of $i_{out} = (v_{in} - 0)/R$ due to its inverting input terminal is at $0 V$. At inverting type, current flows from inverting input to output port of op amp, while the current is same as at non-inverting type, the polarity of the flows is opposite. While inverting type has better voltage compliance with regard to non-inverting type, it also has a disadvantage of not seeing an infinite resistance. Floating types of converters are not suitable for ground required loads. They have stability problems when larger loads are needed to drive. They have also gain problems if there is no adjustable resistor, as

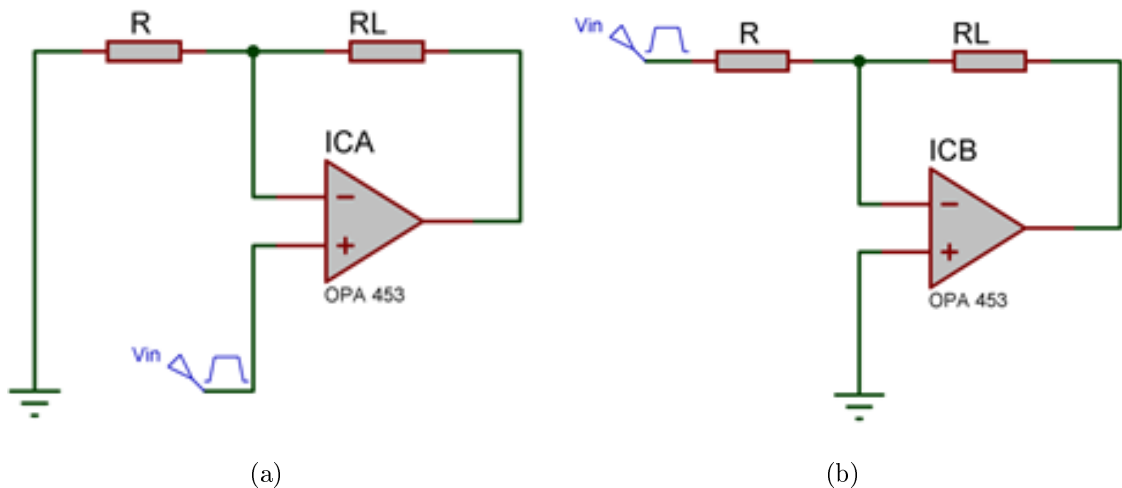


Figure 3.1 Non-inverting Floating-Load V-I Converter (a), Inverting Floating-Load V-I Converter(b).

sensitivity resistor, used in their circuit. On the other hand they are the most basic and easy to construct types of current sources designed with op amps, in general [11].

3.1.2 Grounded-Load Converters

Grounded-load converter means that when one of the terminals of load is committed to ground there is no feedback loop for the op amp. These types of converters are suitable for grounded loads. Figures 3.2 and 3.3 are most common grounded-load converters are Howland and improved Howland current sources that are named after their inventor Prof. Bradford Howland. There are many different types of voltage controlled current source topologies; however, Howland topologies are most practical and preferred types due to convenience of design. In Howland topologies, current can easily be achieved just by using small number of discrete components as resistors. Op amps are high performance components and they have robust characteristics at nerve and muscle stimulations.

- **Howland current pump**

Howland current source consists of an op amp, a set of resistors and an input

voltage to control output current of the circuit. Current flows toward ground through the load. The output resistance, seen by the load, is found by Norton equivalent and eq. 3.4 is achieved [11].

$$R_{out} = \frac{R_2}{R_2/R_1 - R_4/R_3} \quad (3.4)$$

As it is mentioned before, for a correct conversion, $R_{out} = \infty$ is essential so in order to ensure this situation there should be perfect match of resistors as eq. 3.5.

$$\frac{R_2}{R_1} = \frac{R_4}{R_3} \quad (3.5)$$

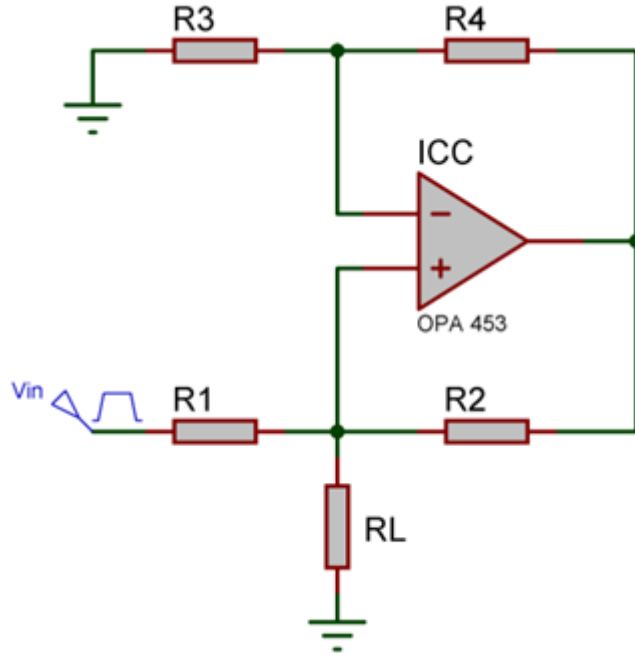


Figure 3.2 Howland current source.

In Howland current source mode, in Figure 3.2, output current is calculated by eq. 3.6 where the gain is $\frac{1}{R_1}$. This equality lay on the eq. 3.5 which is related to $R_{out} = \infty$ condition.

$$i_{out} = \frac{1}{R_1} v_{in} \quad (3.6)$$

When the input voltage v_{in} is positive, the Howland source supply currents to

drive the load otherwise it sinks current. In order for a large range of voltage compliance, R_1 must be greater than R_2 .

- **Improved (Modified) Howland current pump**

In most cases, Howland current source is more wasteful in terms of power in comparison with modified Howland current source. In order to solve this insufficient use of power, the circuit is modified and the R_2 , in Figure 3.2 is divided into two resistors R_{2A} and R_{2B} , in Figure 3.3, whose summation is again equal to R_2 , in eq. 3.7.

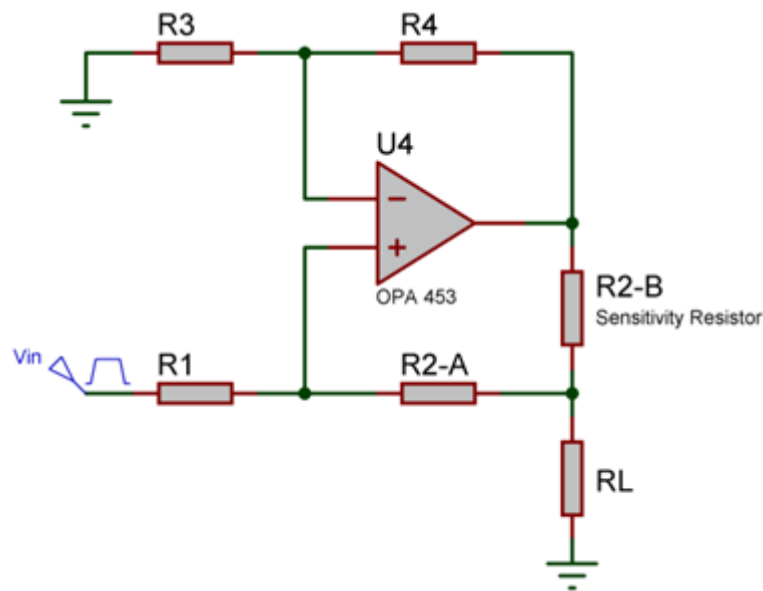


Figure 3.3 Improved Howland current source.

The modification of Howland circuit and splitting R_2 into two resistors does not affect $R_{out} = \infty$ condition because eq. 3.5 just turns to eq. 3.8 and infinity condition is still valid. These modification turns Howland current source to a power saving improved Howland current source whose output current is in eq. 3.9 where R_{2B} is sensitivity resistor which decides output current when divides input voltage. The expression of $\frac{R_2}{R_1}$ adjusts the gain of the circuit. Choosing R_{2B} is small enough can be power savings but in some cases; being too small can result in stability problem on the output current of the circuit.

$$R_2 = R_{2A} + R_{2B} \quad (3.7)$$

$$\frac{R_{2A} + R_{2B}}{R_1} = \frac{R_4}{R_3} \quad (3.8)$$

$$i_{out} = \frac{R_2}{R_1} \frac{v_{in}}{R_{2B}} \quad (3.9)$$

Apart from the sensitivity resistor R_{2B} , other resistors of the circuit can be chosen much greater for higher gain in order to reach high current values when the produced input voltage is small. Improved Howland current source has both positive and negative feedbacks so it can be better for distortion problems at high frequencies if small capacitors are attached parallel on R_1 and R_4 [11].

Effect of resistance mismatches

High precision resistors are strictly essential to avoid resistance mismatches which causes low output resistance. Resistors tolerance values decrease the possibility of resistors are perfectly matched each other and this reduces the R_{out} that is essential for perfect V-I conversion in order to get a constant current output in any value of load [11].

Resistance mismatches can be overcome by high precision resistor trimmers but they are both thermally and mechanically unstable components so high precision typical axial lead resistors, with low tolerance value, are suitable in order to solve this problem.

Maximum load resistance

Maximum load resistance is related to the terms of maximum output current and voltage saturation value (v_{sat}) of the circuit. Eq. 3.11 shows maximum load resistance ($R_{loadmax}$) can be calculated according to desired maximum output currents (i_{outmax}) [19].

$$R_{load\ max} = \frac{R_1 + R_2 A \left[\frac{v_{sat}}{i_{out\ max}} - R_2 A \right]}{R_1 + R_2} \quad (3.10)$$

For instance, our circuit can produce 10 mA_{pp} where $R_{loadmax} = 5.7\ k\Omega$.

3.2 Stimulator Diagram and Analysis

After all theoretical information, this part of document consists what was done during design procedure. At very beginning of the study current studies were analyzed deeply and their convenience was compared to our requirement then their advantages were utilized while disadvantages were avoided. In the light of literature survey, the need of use a power op amp, high voltage supplier, isolation unit, external triggering and a flexible software control unit, were occurred [3].

3.2.1 Power Supply of the System

This is an alternating current (AC) to direct current (DC) converter power supply unit which consists of transformers, rectifier circuits, filters, fuses and regulators. The power supply unit of the system should produce high voltages for power op amp of the stimulator. This unit has three dual power supplying part in it. These give a $\pm 37\ V_{dc}$ and two $\pm 5\ V_{dc}$. In Figure 3.5, there are two different parts of the unit; the above one, in Figure 3.5, supplies $\pm 37\ V_{dc}$ and $\pm 5\ V_{dc}$ where the below one supplies

just $\pm 5 V_{dc}$. These two units are totally isolated.

The power supply of the system has two different transformers that reduce the high ac voltage to a lower ac voltage. First transformer TR1 has a $36 V_{ac} - 0 - 36 V_{ac}$ secondary for supplying $\pm 37 V_{dc}$ via the regulators: LM317K for positive supply and LM337K for negative supply. VA+ is the $\pm 37 V_{dc}$ connected to power op amp's positive supply input where VA- is the $-37 V_{dc}$ connected to power op amp's negative supply input. LM317K and LM337K are three terminal adjustable regulators controlled by a set of resistors and obey the formula of eq. 3.11 where $v_{ref} = 1.25 V_{dc}$ between output and adjustment terminal, $v_{out} = VA+$, $\frac{R_1}{R_3} = 29$ so $v_{out} = +37 V_{dc}$. This is the sample calculation of adjustable regulators used in current study.

$$v_{out} = v_{ref} \left[1 + \frac{R_1}{R_3} \right] \quad (3.11)$$

Second part of the above circuit in Figure 3.5 converts $\pm 37 V_{dc}$ to $\pm 5 V_{dc}$

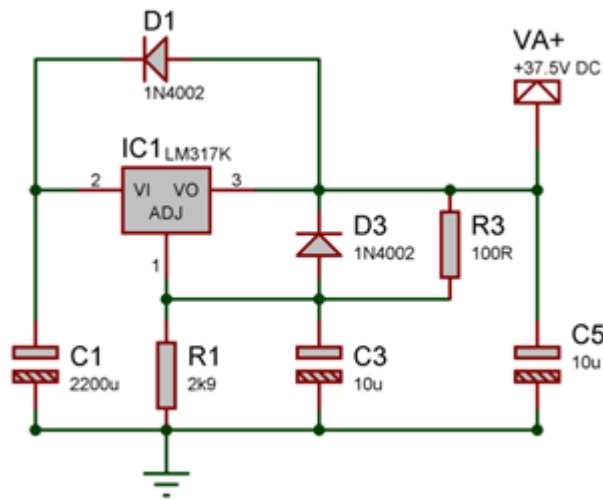


Figure 3.4 The scheme of adjustable regulator of LM317K.

via adjustable regulator (Figure 3.4) but designers should be aware of the minimum and maximum values of adjustable regulators in order not to encounter any stability problem of power supply. Above circuit supply both power op amp for V-I conversion and one part of the isolation amplifier.

Second transformer TR2 has a $7.5 V_{ac} - 0 - 7.5 V_{ac}$ secondary for supplying $\pm 5 V_{dc}$. There is no need of any resistors due to using voltage regulators of LM7805

and LM7905. These are simple regulators which are no need of any adjustment. The below circuit of the Figure 3.5 is for supplying both comparator unit and the other part of the isolation amplifier.

There are also fuses, about 50 mA , for protection from short-circuits or any other electrical problem. Light emitting diodes (LED) are needed for indication if there is a problem on the circuit or not.

3.2.2 Isolation Amplifier and Current Source

This part of the document creates the infrastructure of the thesis and also it is the main circuit of all system designed and produced for the purpose of getting an isolated computer-controlled constant-current source. This part is divided into two groups where the essential steps of design procedure are mentioned. First part covers the isolation unit and an RC low-pass filter while the second part covers the V-I converter.

• Isolation Amplifier and Low-Pass Filter

Isolation is an essential and vital issue for electrical safety which has a fatal significance on living tissues. Isolation amplifier is used in order to reduce artifacts and supply higher safety condition during current stimulation. Isolation amplifier isolated the load from power supply and output of personal computer soundcard. ISO 124 IC is a unity gain isolation unit used in this study as isolation amplifier. ISO 124 transmits the signal by modulation-demodulation technique via a capacitive barrier. Isolation amplifier act as a linear amplifier up to 250 kHz of input signals but small-signal bandwidth is lower than it such as 50 kHz . Power supply pins of the ISO 124 should be by passed by $1\ \mu\text{F}$ tantalum capacitor due to noise problem of supply can cause unstable output signal but tantalum capacitors should be paid attention because tantalum capacitors causes many problems in electronic circuits [3].

Output of isolation amplifier has a ripple voltage of $20 - 30\text{ mV}$ at 500 kHz

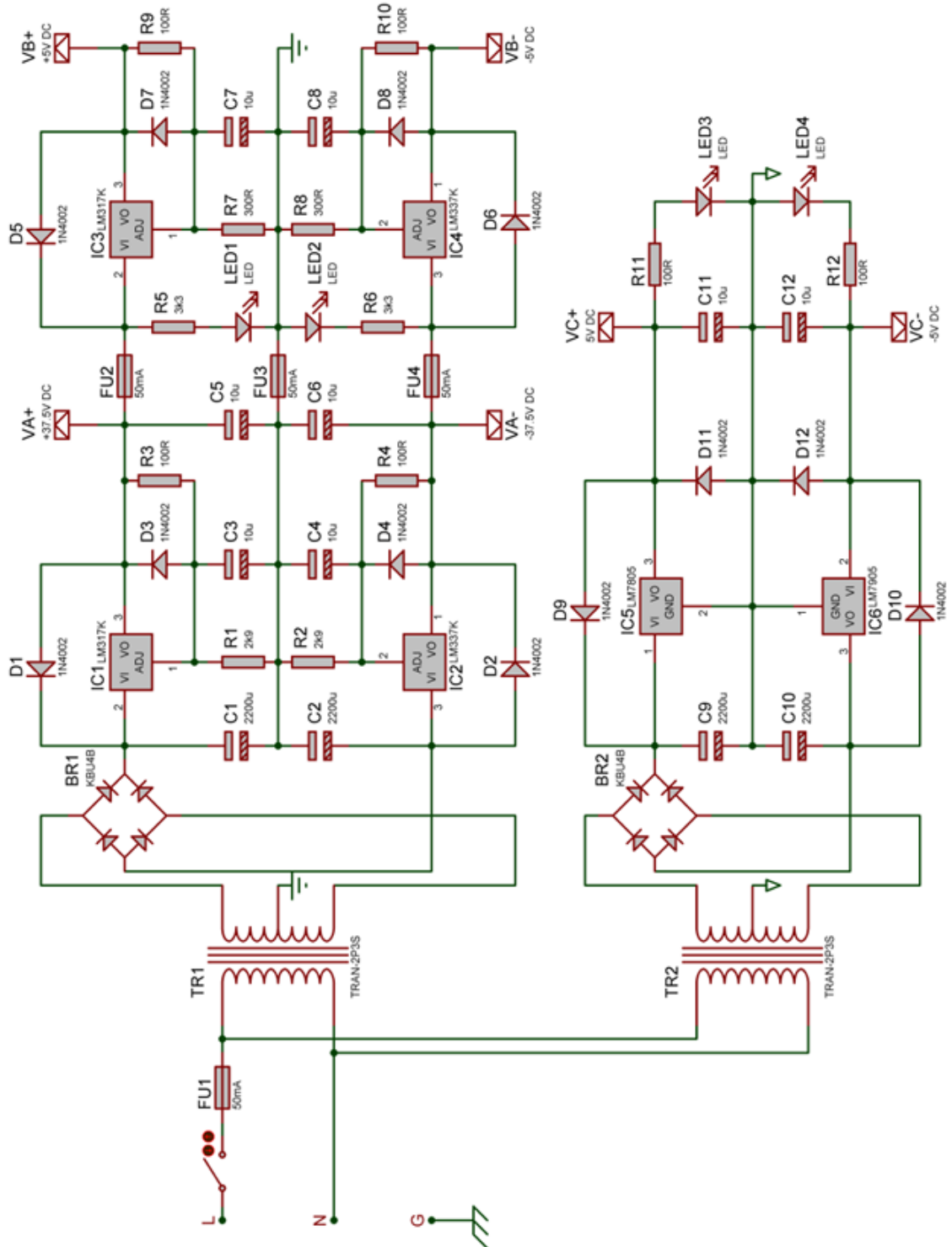


Figure 3.5 The circuit scheme of power supply unit of the stimulator. The power supply unit includes 3 independent dual-power supplies.

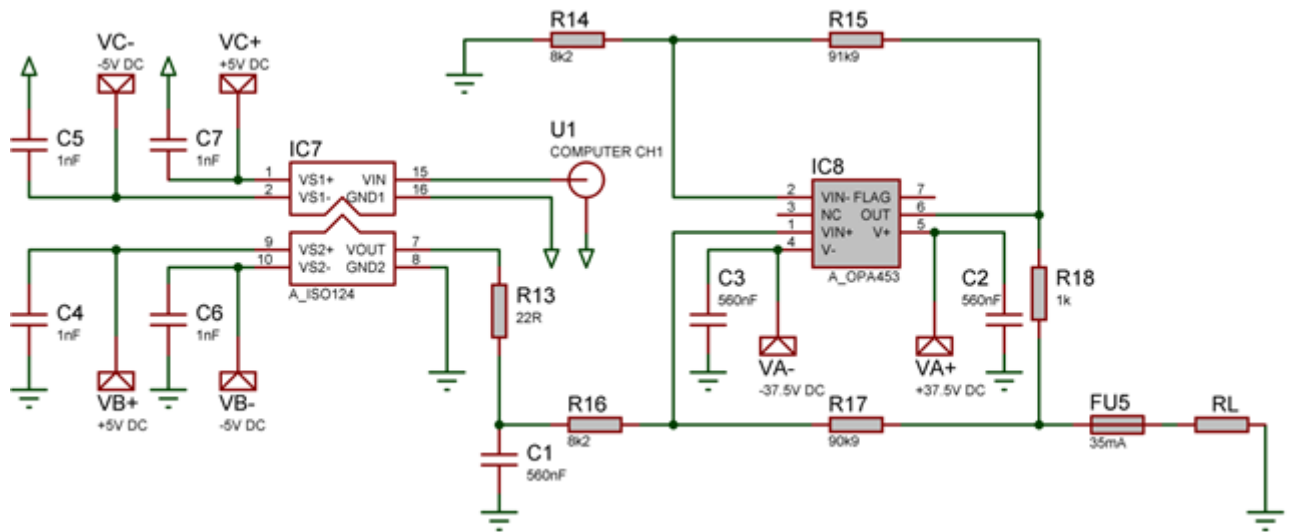


Figure 3.6 Stimulator circuit schemes which consist of isolation amplifier, RC low-pass filter and improved Howland current pump.

due to modulation-demodulation so when this signal with ripples amplifies by power op amp by means of gain about 11.2, this noise reaches 200 – 300 mV and it is an undesired situation while working small input signal so we applied a simple RC low pass filter (Figure 3.7) whose cut-off frequency is about 13 kHz .

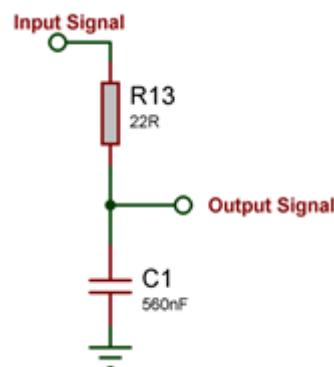


Figure 3.7 RC Low-Pass Filter.

- **Voltage to current converter**

At the beginning of all, we tried basic floating type V-I converters due to easiness of design and setup. However floating load V-I converters are easily setup, they

have gain and stability problems at output current. At the second step we analyzed Howland current source which gives a constant current but it spends more power while modified (improved) Howland current source is energy efficient when compared to Howland topology.

Howland topologies are advantageous over other V-I converters due to no need of additional discrete components transistors, diodes if the output current will not be boosted up. Choosing a power op amp and a dual power supply provides both high voltage compliance and this match also produces biphasic currents as positive and negative. Howland topologies also overcome crossover distortions and transconductance mismatches. Howland topologies can bring reliable constant current when the resistors are matched perfectly, this is the most important necessity for Howland circuits.

Input bias and offset currents affect the output current so a precision amplifier whose input offset current is low enough should be used in a Howland current source circuit. Slew rate is the ability of an op amp to respond as fast as when the input signal is changed. R_2 and R_4 should be reduced in order to increase the slew rate of the stimulator. These resistors also affect the bandwidth in a good way when they are chosen smaller in value. But, on the other hand when we make them so smaller, the gain of the system becomes low and output current cannot reach the desired value due to the maximum value of the input signal is not very high. These situations are considered during the design procedure and OPA 453 - Power Op Amp (80 V, 50 mA) of the Texas Instruments is decided to use. OPA 453 is a high output load drive about 50 mA with a wide bandwidth of 7.5 MHz and needs a gain term at least 5 or greater [20].

Input signal can be applied to either non-inverting input or inverting input. When the input signal is applied to non-inverting input we get high voltage compliance but on the contrary when it is applied to inverting input low distortion is provided. In this study high voltage compliance is chosen [20].

At the beginning of the design, we used small value resistors which cause some stability problems on output currents. Sensitivity resistor should be high at least it should be greater than 500 Ω if it is not so there occurs some failure on the output current when the loads become high about 20 – 25 k Ω . The op amp specification is that the gain of the system should be equal or greater than 5 so our resistor values are;

91.9 $k\Omega$ and 8.2 $k\Omega$ (1% metal film resistors).

A couple of set of resistors are tried in order to find the best matches of all and to produce the best quality of constant current output for driving biological loads reliably. High precision resistors (i.e. 0,025% – 0,01%) are so difficult to find to buy in the domestic market. The best tolerance quality in precision is 1% so we used metal film resistors with 1% tolerance. As we mentioned before resistor mismatches cause serious problems such as decline of output current at larger loads, instability of the signal or low output resistance. Each of the resistors is chosen by one by one by measuring the exact value of the resistors by a multimeter to provide a perfect match.

Output resistance of the circuit which is seen by the load should be high enough to be able to drive load by a constant current that is stable and not change with the load resistance variation. According to Eq. 3.4 $R_{out} = \frac{R_2}{R_2/R_1 - R_4/R_3}$, shows formulation of how output resistance is calculated, $R_{out} = \infty$ when the resistors are precise and perfectly match with each other ($R_2/R_1 - R_4/R_3 = 0$). This is true in theory but in reality R_{out} can just converge to infinity so R_2 should be high enough to provide a greater output impedance at any load resistance.

If the system was forced to run under high frequency range so there occurred a need of placement of capacitors as parallel with both R_1 and R_4 but on the other hand this could cause slowing down of responses.

In improved Howland topology, load resistance R_L should not affect the output current i_{out} in the range of power op amp specifications (Figure 3.8). The output current is calculated by the eq. 3.12 whenever eq. 3.13 is provided.

$$i_{out} = \frac{R_4}{R_3 R_{2B}} \quad (3.12)$$

$$R_3(R_{2A} + R_{2B}) = R_1 R_4 \quad (3.13)$$

Output current of the circuit in Figure 3.8 is eq. 3.12 In order to achieve it we applied Kirchhoff current law. We also used general op amp design knowledge of no

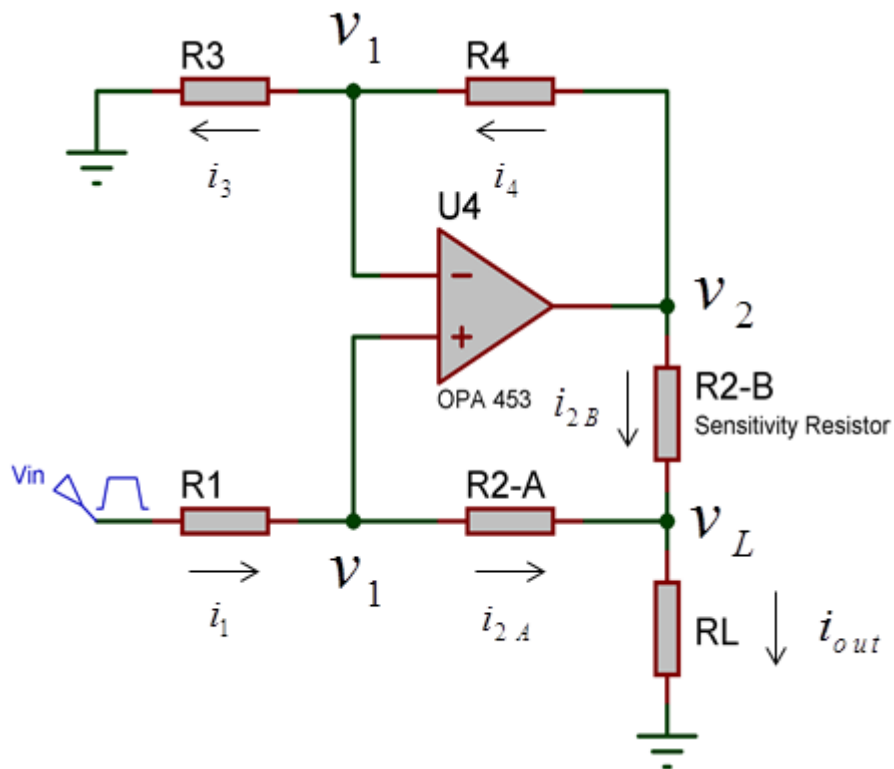


Figure 3.8 Improved Howland Current Source.

current flows both input terminal of op amp. Output current i_{out} flows on R_L causes v_L . There are three unknown parameters, on Figure 3.8, v_1 , v_2 and v_L . In order to make i_{out} is independent from R_L we will eliminate R_L [19].

$$v_L = i_{out}R_L \quad (3.14)$$

First, node equations are written in terms of current law and then ohm's law is applied in order to define the term in terms of voltages. This is followed in eq. 3.15, 3.16 and 3.17.

$$i_4 - i_3 = 0 \rightarrow \frac{v_2 - v_1}{R_4} - \frac{v_1}{R_3} = 0 \rightarrow v_2 = v_1 \left[1 + \frac{R_4}{R_3} \right] \quad (3.15)$$

$$i_1 - i_{2A} = 0 \rightarrow \frac{v_{in} - v_1}{R_1} - \frac{v_1 - v_L}{R_{2A}} = 0 \rightarrow v_1 = \frac{v_{in}R_{2A} + v_L R_1}{R_1 + R_{2A}} \quad (3.16)$$

$$i_{2B} + i_{2A} - i_{out} = 0 \rightarrow \frac{v_2 - v_L}{R_{2B}} \frac{v_1 - v_L}{R_{2A}} - i_{out} = 0 \quad (3.17)$$

Equations 3.14, 3.15 and 3.16 is added to 3.17 so;

$$v_{in} \left[\frac{R_3(R_{2A} + R_{2B}) + R_4 R_{2A}}{R_3 R_{2B} (R_1 + R_{2A})} \right] = i_{out} \left[\frac{R_L [R_3(R_{2A} + R_{2B}) - R_1 R_4]}{R_3 R_{2B} (R_1 + R_{2A})} + 1 \right] \quad (3.18)$$

$$R_3(R_{2A} + R_{2B}) - R_1 R_4 = 0 \quad (3.19)$$

To get i_{out} is independent of R_L the term $R_3(R_{2A} + R_{2B}) = R_1 R_4$ should be achieved. $R_1 R_4$ expression is substituted by $R_3(R_{2A} + R_{2B})$ in eq.3.18 in order to simplify i_{out} expression so;

$$i_{out} = v_{in} \left[\frac{R_4 (R_1 + R_{2A})}{R_3 R_{2B} (R_1 + R_{2A})} \right] \quad (3.20)$$

is achieved then the final term (eq. 3.12 $i_{out} = \left[\frac{R_4}{R_3 R_{2B}} v_{in} \right]$) is reached. In this expression, the term $\frac{R_4}{R_3}$ shows the gain of the system while R_{2B} is the sensitivity resistor which determines the output current conversion.

The above equation (eq. 3.12) gives the output current i_{out} of a classical improved Howland current source which is one of the popular V-I converter topologies.

3.2.3 Comparator for External Devices

Comparators have been used for many applications such as level detectors, on-off controller, window detectors, bar graph methods, pulse-width modulation and more other areas. In this study, comparator is used for triggering an external device in order to amplify and record data from laboratory animal when the biological experiment is performed. The comparator of this study produces 5 V - TTL that is compatible with external device's (Micromed Amplifiers) trigger input.

In this study, LM 311 - Single comparator is chosen as the IC for this study due to properties such as low input current voltage, dual or single supply voltage, low input bias-offset currents and response time.

The main basis of voltage comparator (Figure 3.9(a)) is to compare the two independent input voltages at positive input pin V_{IN+} (voltage at non-inverting input) with respect to negative input pin V_{IN-} (voltage at inverting input) and when the voltage at positive input pin is higher than negative input voltage so the output voltage is decided as high V_{OH} , on the contrary it becomes low V_{OL} , (Figure 3.9(b)) [19].

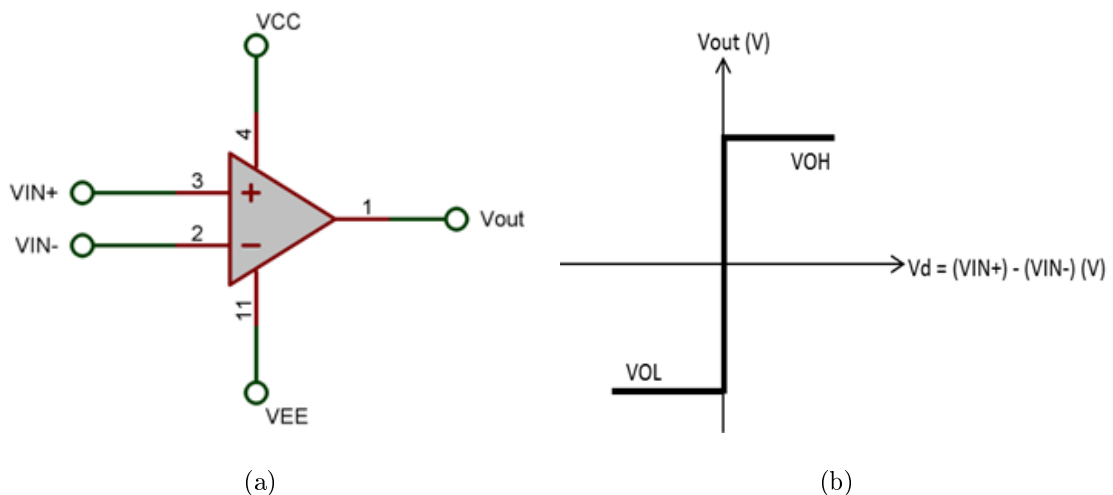


Figure 3.9 Basic symbol of a comparator (a), Voltage transfer curve of a comparator (b).

Differential input voltage (v_d) is equal to difference of Positive and negative input voltages ($V_{IN+} - V_{IN-}$).

$$v_{out} = v_{OL} \text{ for } v_{in+} < v_{in-} \quad (3.21a)$$

$$v_{out} = v_{OH} \text{ for } v_{in+} > v_{in-} \quad (3.21b)$$

Response time of a comparator is a significant figure for responding the changes at the input stage of the comparator. In some applications, especially when two or more systems are running parallel, being speedy is needed in order not to be late to reply changes at input stages. Response time can decrease or increase with respect to input voltages and device characteristics. The device, used in current study, is LM 311 whose response time (200 ns) is suitable for current system of this paper. An op-amp can be a great comparator when speed is not vital. Here our comparator monitors a threshold value to control output of comparator for driving an external device. There is LED on comparator as an activation indicator.

A comparator is an open-collector output device whereas the op-amps are push-pull output devices so op-amps swing between their supply ranges where the comparators have a flexible output stages. An external pull up resistor is placed between output pin and a voltage source (+5 V DC) which is desired at the output of the comparator when the output is high VOH [11, 21].

A non-inverting comparator use two resistors for generating hysteresis and this is smaller in number than inverting ones.

$$R_{pull-up} < R_{load} \quad (3.22)$$

$$R_{20} < R_{pull-up} \quad (3.23)$$

- R_{20} resistor is placed in figure 3.10.

Large pull up resistors reduce the maximum output voltage on the contrary if the pull up so small it cannot supply enough voltage and current to output stage so the eq. 3.22 and 3.23 should be considered as design specification.

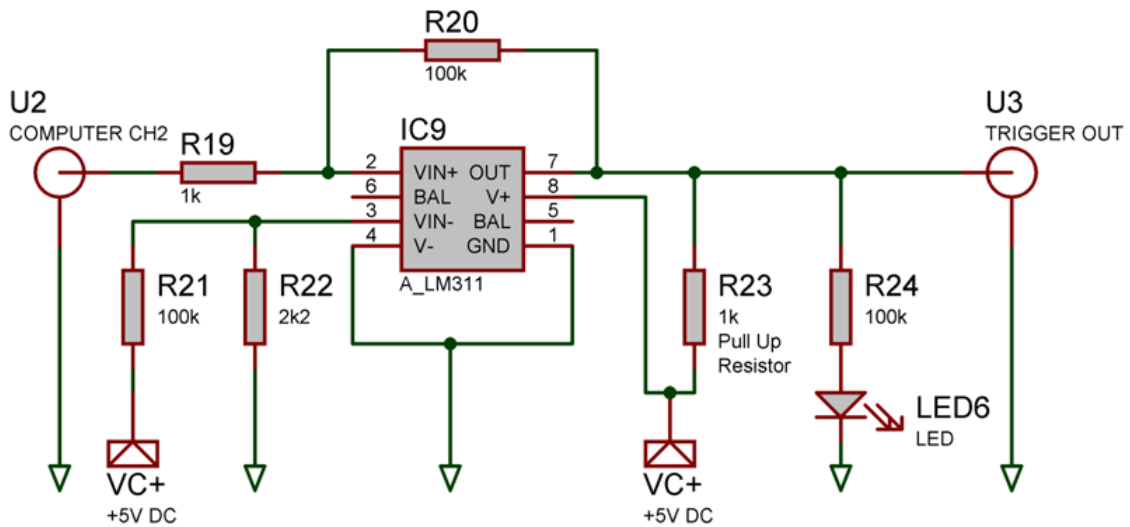


Figure 3.10 Comparator circuit: generate 5V TTL for triggering external device.

- **Hysteresis**

Hysteresis prevents the comparator from unintentional on-off switching which can be caused by electrical noise or any other factors. There is 50 *mV* hysteresis in comparator unit of this study. Hysteresis can be achieved when the threshold of on-to-off switching is lower than the off-to-on switching. Hysteresis is a safety range when a system processes with small signal values. The input voltage on the non-inverting input should be higher than the reference voltage at the inverting input stage for high output voltage (Figure 3.11) [3, 22].

$$\text{Hysteresis} = \Delta v_{in} = v_{in}^{+} - v_{in}^{-} \text{ or } \text{Hysteresis} = \Delta v_{threshold} = v_{TH} - v_{TL}$$

For threshold is **high** where the output of the comparator is **low** means that output equals to negative supply of the comparator $v_{ee} = 0V$ (*grounded*).

$$\text{For } v_{in}^{+}; \frac{v_{in} - v_{ref}}{R_{19}} = \frac{v_{ref} - v_{ee}}{R_{20}}$$

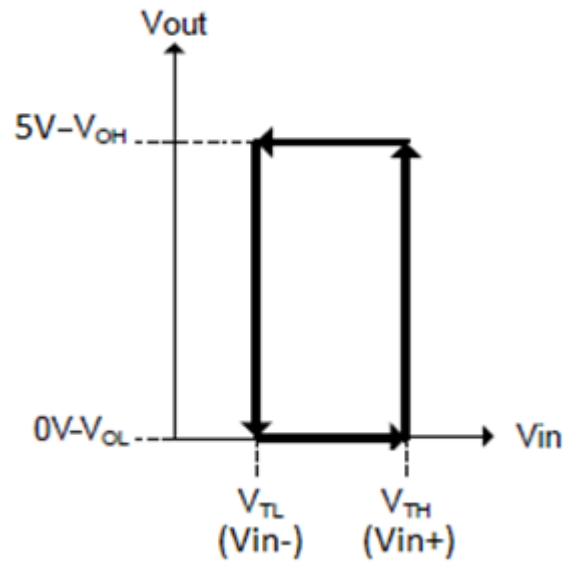


Figure 3.11 Voltage transfer curve of the current comparator where $v_{TH} = 0.0109 V$ and $v_{TL} = 0.059 V$.

$$v_{in} = \left[\frac{v_{ref}(R_{19} + R_{20})}{R_{20}} - \frac{R_{19}v_{ee}}{R_{20}} \right]$$

For threshold is **low** where the output of the comparator is **high** means that output equals to positive supply of the comparator $v_{cc} = 5V$.

$$\text{For } v_{in}^-; \frac{v_{in} - v_{ref}}{R_{19}} = \frac{v_{ref} - v_{cc}}{R_{20}}$$

$$v_{in} = \left[\frac{v_{ref}(R_{19} + R_{20})}{R_{20}} - \frac{R_{19}v_{cc}}{R_{20}} \right]$$

So, we calculate the hysteresis as follow;

$$v_{in}^+ = 0.109 V \text{ and } v_{in}^- = 0.059 V$$

$$Hysteresis = v_{in}^+ - v_{in}^- = 0.109 V - 0.059 V = 0.05 V$$

Where $v_{ref} = 0.108mV$ by the voltage divider rule while resistors ratio;

$$v_{ref} = 5 V \frac{2.2k\Omega}{102.2k\Omega}$$

3.3 Computer Interface and Software

The system is controlled via an internal soundcard of a personal computer. A soundcard device can produce $3.5V_{pp}$ amplitude in the range of $10 - 20,000 Hz$ frequency. Soundcards are divided into two groups such as mono and stereo. The soundcard of the personal computer which is used in this study in order to control the circuit is a stereo one. A stereo soundcard has two channels, right and left or channel 1 and channel 2, that means a soundcard can drive to circuits in parallel but independently.

LabVIEW is graphical software program where many things are easily tied each other and a controller or any other program can be created (Figure 3.3 and 3.15). LabVIEW is developed by National instrument. We developed two different programs which are used for biological tests (Figure 3.12) and electrical tests (Figure 3.14).

For the biological test we design a pulse generator which controls the amplitude-current value, pulse width and delay time. Pulse generator uses two channels of soundcard. One of the channels activates comparator and the other one activates the stimulator. For comparator triggering the software is arranged to $500 mV$ and $10 ms$ which means channel 2 gives $500 mV$ voltage during $10 ms$ and the external devices will be triggered along $10 ms$ to record biological data. On the other hand, stimulator software can produce $50 - 10,000 \mu A$ reliably along $50 - 100,000 \mu s$.

For the electrical test we design a waveform generator which generates sinusoidal, square and triangular waveforms to electrically test the stimulator. In this part of software, we did not divide the channels due to no need. We tested the device with

sinusoidal waveform at maximum and minimum values that can be produced by sound-card which are $10 - 20,000 \text{ Hz}$ and $3.5 V_{pp}$ means that device can produce 6.6 mA_{pp} for $10 \text{ k}\Omega$ dummy load.

The results of electrical and biological tests are given at chapter 4.

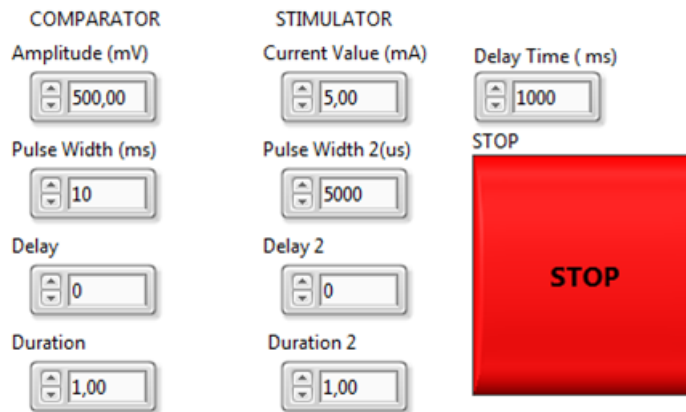


Figure 3.12 Front panel, for user interface, of the LabVIEW software for generating pulses both for stimulator and comparator units of the system.

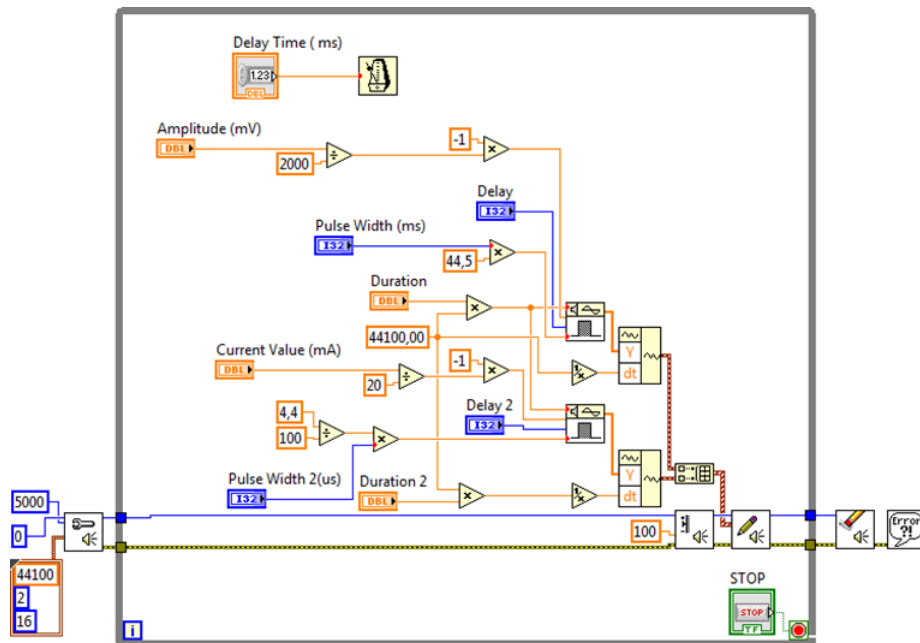


Figure 3.13 Block diagram of the LabVIEW software for generating pulses, by independently controlling two channels of internal soundcard of a computer, both for stimulator and comparator units of the system.

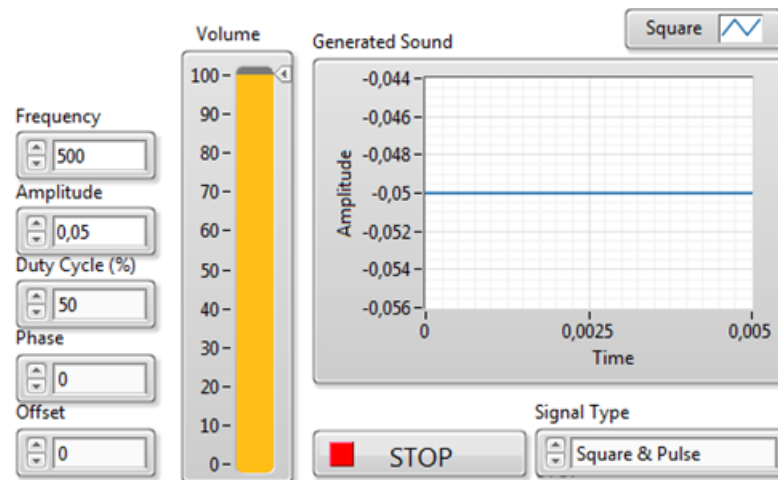


Figure 3.14 Front panel, for user interface, of the LabVIEW software for generating waveforms in order to electrically test the stimulator system.

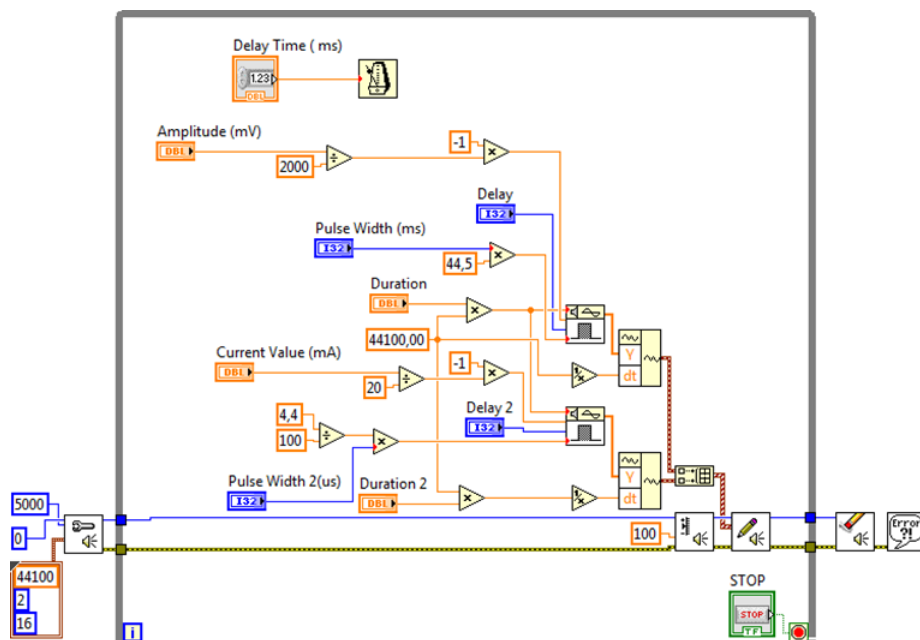


Figure 3.15 Block diagram of the LabVIEW software for generating waveforms, by controlling internal soundcard of a computer, in order to electrically test the stimulator system.

3.4 Electrode Selection

Somatosensory evoked potentials are recorded after applying electrical stimulation via electrodes to peripheral sensors by subcutaneously. Stainless steel needle electrodes are commonly used in these studies. Biphasic types of waveforms are offered to select in order to decrease ion transfer and electrode polarization but in this study, pulse stimulus are chosen for just excite the peripheral nerves at the left toe (related to posterior tibial nerve) Somatosensory evoked potentials are recorded after applying electrical stimulation via electrodes to peripheral sensors by subcutaneously. Stainless steel needle electrodes are commonly used in these studies. Biphasic types of waveforms are offered to select in order to decrease ion transfer and electrode polarization but in this study, pulse stimulus are chosen for just excite the peripheral nerves at the left toe (related to posterior tibial nerve) [14].

4. RESULTS

This chapter includes results of electrical tests and biological experiment of the device. Two topics exist here and they are analyzed in detail. The titles of the subtopics, respectively, are; calibration and electrical test, and biological experiment.

4.1 Calibration and Electrical Tests

Until now, many of the parts of the document were mentioned such as isolated power supply, isolated stimulator unit, and a comparator unit for external triggering. These systems need a trigger in order to start running. This trigger is the controller unit of the system which can be provided by a sound card of a computer. Here we use a Lenovo V570c computer and its sound card where the limitations of the sound card are $10 - 20,000 \text{ Hz}$ for frequency and $3.5 V_{pp}$ for amplitude. Personal computer's sound card has a linear output as it is showed at Figure 4.1. Experimental results of the system measured via Tektronix TDS 2002C oscilloscope which has a range of 70 MHz frequency and 1 GS/s sampling rates.

Electrical tests are performed where the load is a $10 \text{ k}\Omega$ dummy load (1% metal film resistor). Dummy load is large and its value is close the resistance of dry skin but the resistance of experimental biological tissue is much below $10 \text{ k}\Omega$ so dummy load is chosen high to see the maxima of the device. Input-output function is achieved by setting the software constant at 500 Hz sinusoidal wave and the amplitudes vary by the user interface.

Figure 4.2 shows the input-output response of the stimulator itself when it is driven by software via sound card. Stimulator has a linear output until the system reaches maximum voltage suppliment where the Op amp also saturates at $66 V_{pp}$. Sound card frequency response is shown at Figure 4.3. Device has a flat output in the range of $10 - 20,000 \text{ Hz}$. A sound card can generate signal until $20,000 \text{ Hz}$ but low-pass filter of the stimulator system has a cut-off at $16,000 \text{ Hz}$ so the range is low-

ered. Pulse duration is set in the software between $0,05 - 10 \text{ ms}$ but sound card range can reach 100 ms . Range of frequency supply changes according to the experimental procedure demands. Figure 4.4 shows the frequency response of the stimulator gain almost constant across the range. Figure 4.5 is the frequency response of the entire system from software to output current of the stimulator.

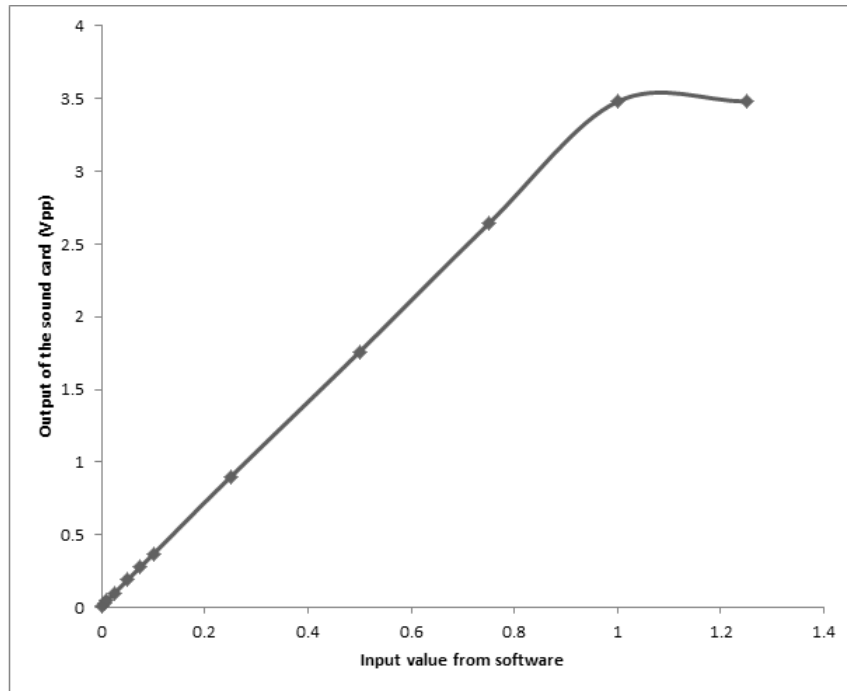


Figure 4.1 Sound card calibration at 500 Hz.

As the device is a current source so its output resistance should be infinity in theory but it is not in reality. This means that the output current of a current source is only approximately constant and may change by various values of load resistance. In order to provide a better constant current condition, equation 3.13 should be satisfied and resistors should match equally. In figure 4.6, output currents changes with respect to increasing load. However in biological applications the load resistance is expected to be lowered. In Figure 4.7 shows that output current is practically constant for loads smaller than 2500Ω .

Figure 4.8 and Figure 4.9 show the output of the sound card for generating positive pulses or periodic waveforms. Positive pulses can be generated and both its pulse width and amplitude can be controlled from the user interface (Front panel of LabVIEW Figure 3.12). Waveforms are generated and their amplitude, frequency and

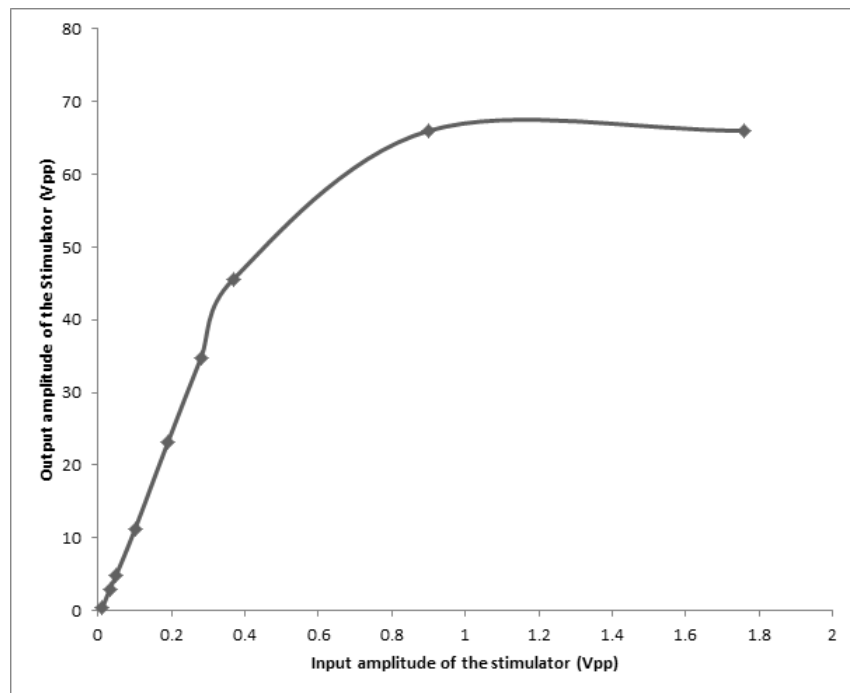


Figure 4.2 Stimulator calibrations at 500Hz with $10\text{k}\Omega$ load.

duty cycle, if it is needed, can be controlled and scaled via user interface (Front panel of LabVIEW Figure 3.14). Figure 4.8 and Figure 4.9 indicate two channels of sound card give outputs independently that is needed during stimulation of biological tissue; the yellow ones drive the stimulator for current injections to tissue where the blue ones activate comparator for external triggering in order to amplify and record data from biological tissue.

In some cases (mostly functional electrical stimulation) biphasic stimulation of biological tissues is essential due to no accumulation of positive or negative ions. Our system can supply biphasic pulses as well [23]. Below figures, Figure 4.10 to Figure 4.13, show both input signal from sound card (yellow) and amplified output signal that is current output (blue) where the load is $10\text{ k}\Omega$.

The ripples, produced by isolation unit and other units, are about $20 - 30\text{ mV}$ and they are mostly filtered by RC low-pass so this situation should be considered while evaluating the relationship between input-output signals on the figures above.

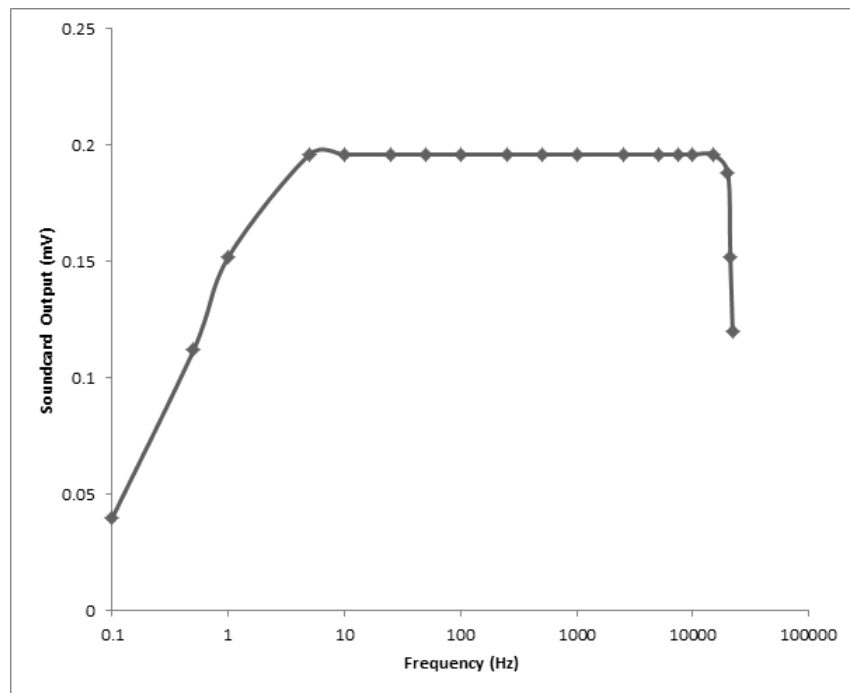


Figure 4.3 Sound card frequency response with 0.05 arbitrary unit set at software.

4.2 Biological Experiments

In this part of the chapter, we analyzed the biological experiment performed to test the device if it is suitable for laboratory use. The experiment was performed on a female Wistar albino rat that (Weight: 204 gr - Birth: 27.09.2013 - Experiment Day: 03.06.2014). Animal was obtained from the Vivarium of Boğaziçi University and the experiment was approved by the local ethics committee. The rat is kept under conventional conditions such as temperature ($21 \pm 3 C^\circ$) and humidity ($55 \pm 5\%$). Water and pellet diet was provided [14].

Before the experiment, rat was anesthetized with Ketamine/xylazine ($50mg/kg$ ketamine + $10mg/kg$ xylazine). The agents were injected two times in an hour. Sub dermal stainless steel needle electrodes were placed at the left ankle to electrically stimulate the posterior tibial nerve. Somatosensory evoked potentials were recorded by stainless steel electrodes in a sub dermal electrode at the scalp over the somatosensory cortex. An earth ground electrode was connected to the left forefoot. Constant current pulses of $2 - 10 mA$ with duration $100 - 250 \mu s$ were delivered at the rate of 1Hz. The evoked responses were averaged within $50 ms$ period. A commercial ampli-

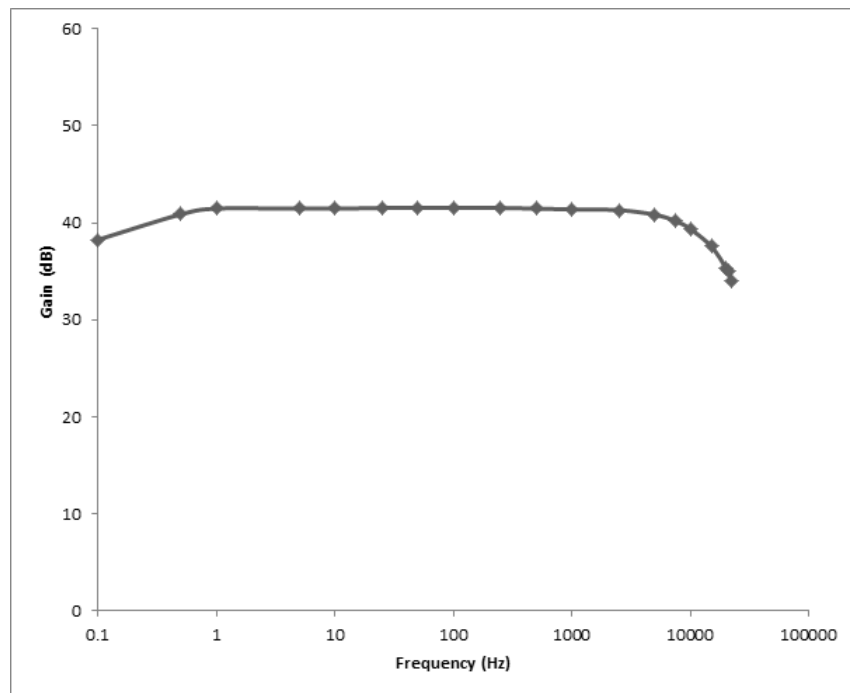


Figure 4.4 Frequency response of the stimulator at 0.05 input value of software with $10k\Omega$ load.

fier, (Micromed) was used for measuring the evoke responses and for averaging data respectively 100, 400 and 370 (Figures 4.14, 4.15 and 4.16). Latencies and peak-to-peak amplitudes were compared to those reported in the literature. The parameters measured are given in Table 4.3 and 4.5. Those from Hayton et al. [14] are given in Table 4.2 and 4.4.

Table 4.1

Comparison of Stimulation parameters of experiments Hayton et al. vs. Current Study.

Stimulation parameters	Hayton et al. (1999)	Current study 1 (SEP1 & SEP2)	Current study 2 (SEP1 & SEP2)
Current Intensity (mA)	1-2	2	10
Duration (ms)	0.1	0.1	0.25
Frequency / pps	3	1	1

As can be seen from Table 4.2 and 4.3 our latencies were slightly lower than those reported in Hayton et al. [14]. Although the stimulations parameters were similar in

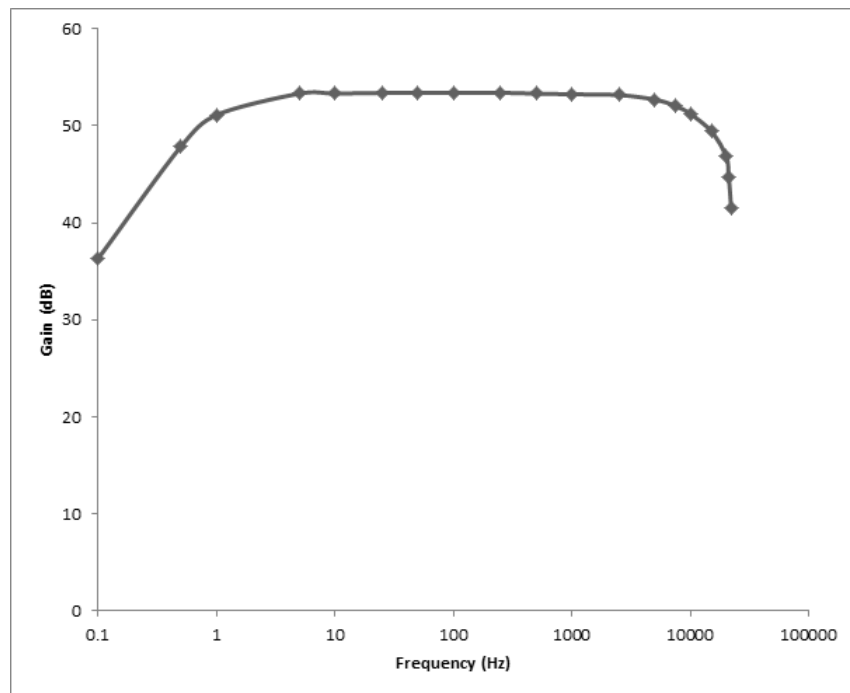


Figure 4.5 Frequency response of the entire system at 0.05 input value of software with 10 k Ω load. Gain calculated according to the equation of $Gain(dB) = 20 * \log(\frac{V_{out}}{\text{Arbitrary unit of software}})$.

both studies, on Table 4.1, the electrodes locations were somewhat different. Hayton et al. stimulated right ankle, we stimulated left ankle and they have 8 subjects. The values given in table 4.2 are averages of those 8 subjects. In addition the amount of anesthetic agents also affects latencies. Hayton et al gave a much higher dose initially which may have prolonged the latencies a little bit. On the other hand, the results on the table 4.4 and 4.5 shows that our amplitude values are much smaller than those reported by Hayton et al. this may be due to the placement of scalp electrodes which we didn't critically control by using an atlas, because our main aim was to demonstrate the use of the stimulator. Additionally we gave extra doses of anesthesia later to complete the experiment this may have reduced the amplitudes, but this does not explain the decrease in the latencies.

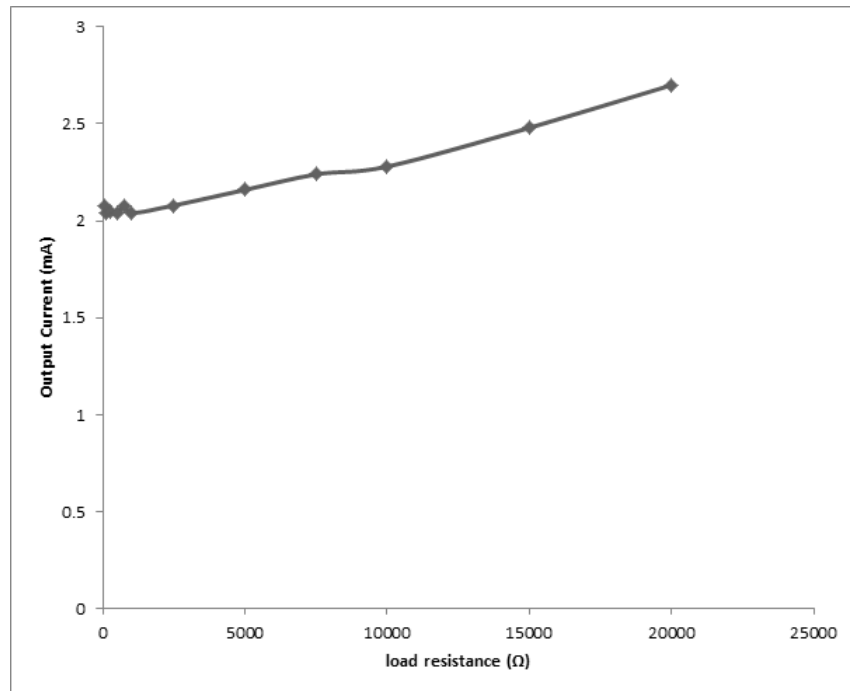


Figure 4.6 The relation between the varying dummy loads and currents values at 500 Hz frequency and 0.05 input value.

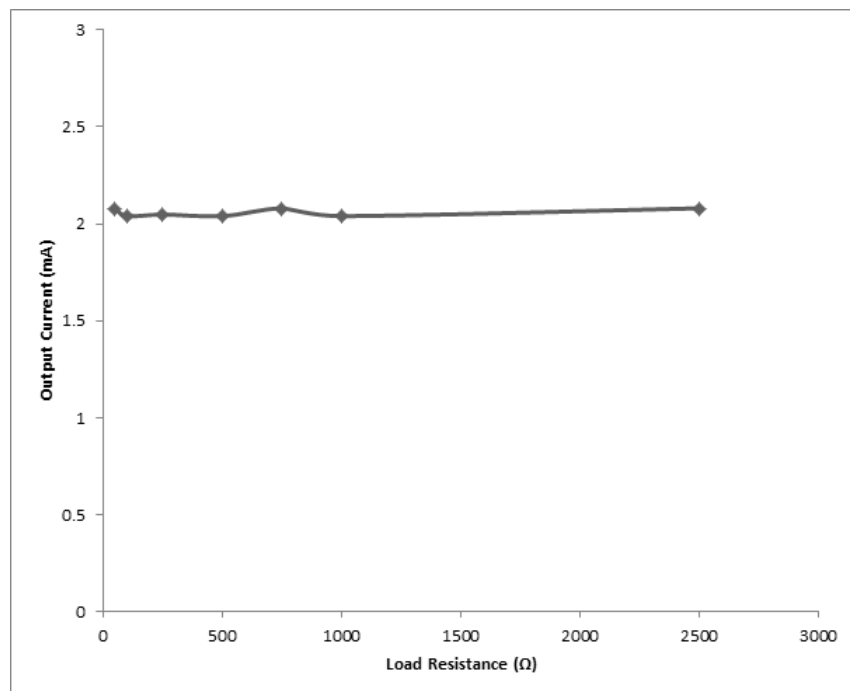


Figure 4.7 The relation between the varying dummy loads, between 50 Ω – 2500 Ω and output current values at 500 Hz frequency and 0.05 input value of software.

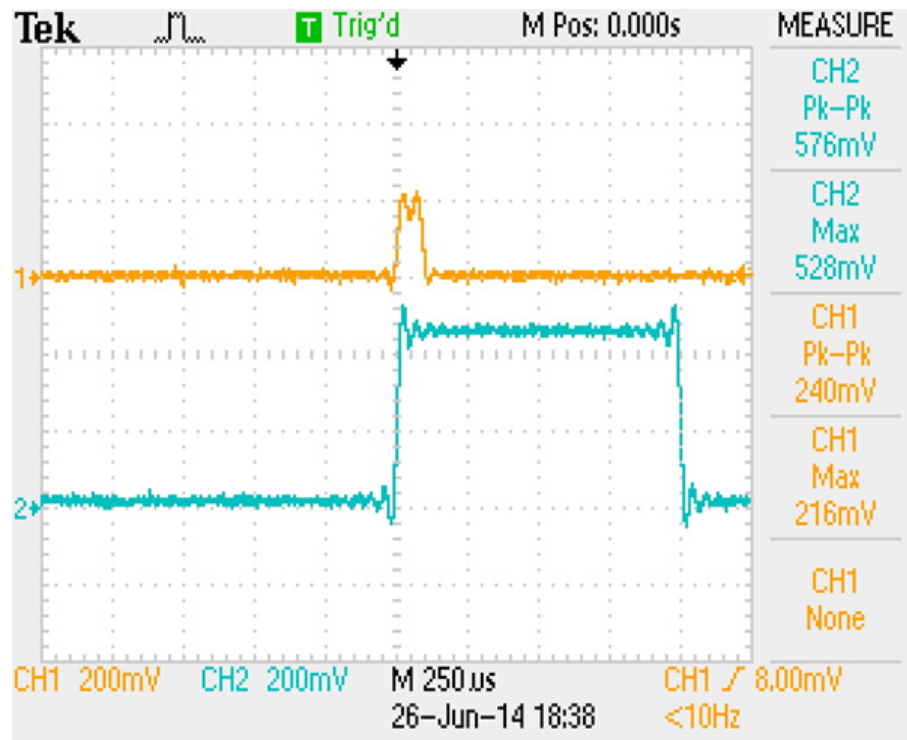


Figure 4.8 100 μs and 216 mV (yellow) and 1000 μs and 528mV (blue) pulses are generated as the output of the sound card in order to trigger both the current stimulator and the comparator.

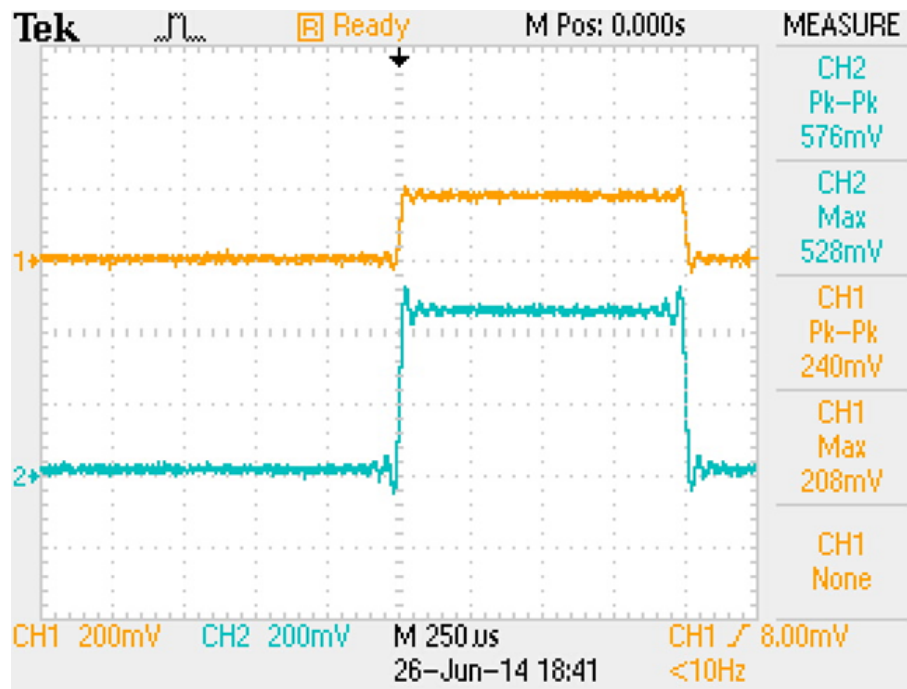


Figure 4.9 1000 μs and 208 mV (yellow) and 1000 μs and 528mV (blue) pulses are generated as the output of the sound card in order to trigger both the current stimulator and the comparator.

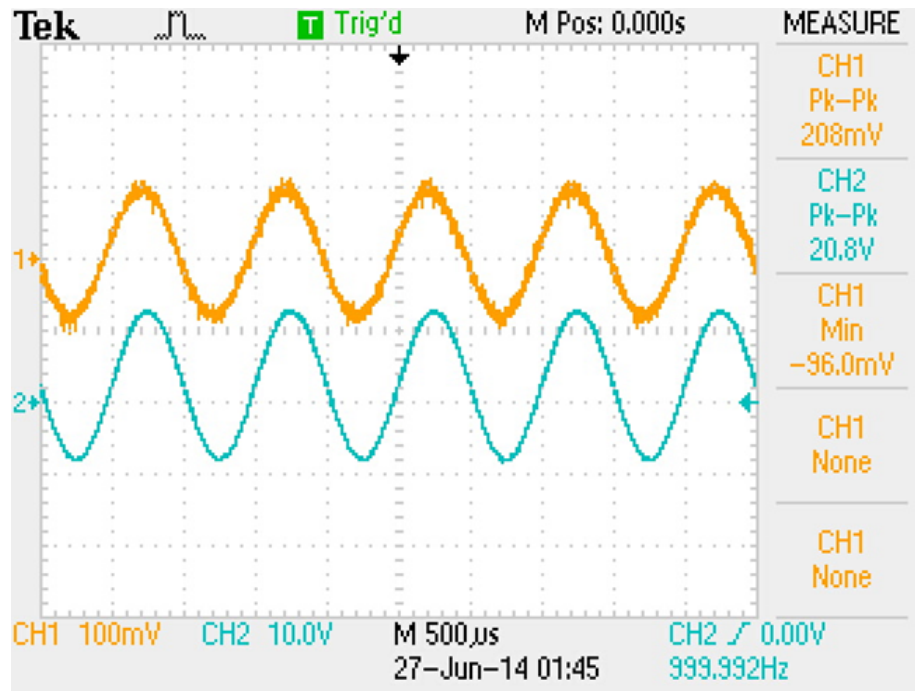


Figure 4.10 Input signal is at 1000 Hz and 208 mV_{pp} where the output signal is at 1000 Hz and 20.8 mV_{pp} .

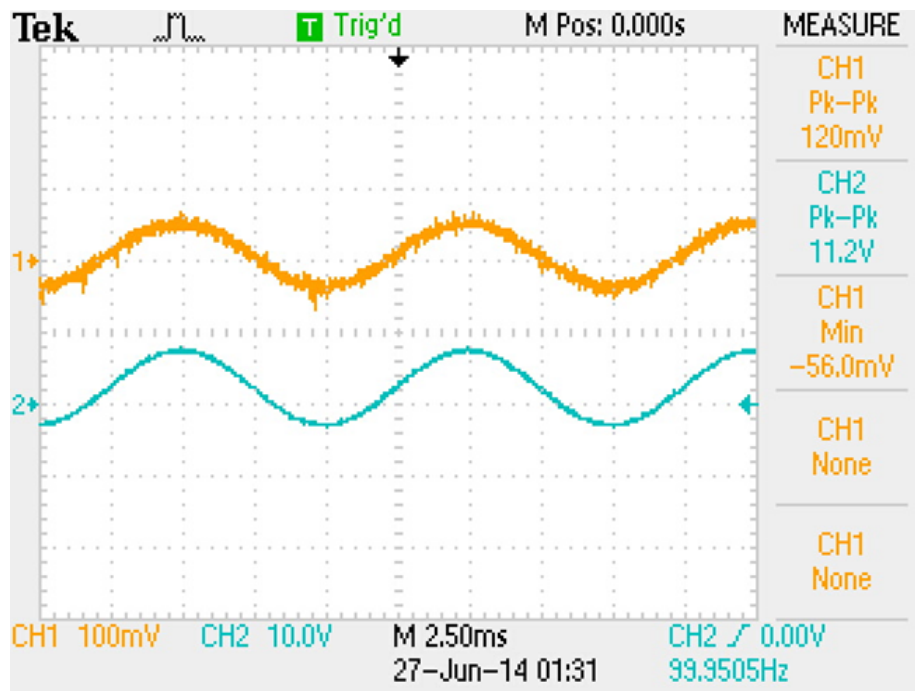


Figure 4.11 Sinusoidal input signal is at 100 Hz and 120 mV_{pp} where the output signal is at 100 Hz and 11.2 V_{pp} .

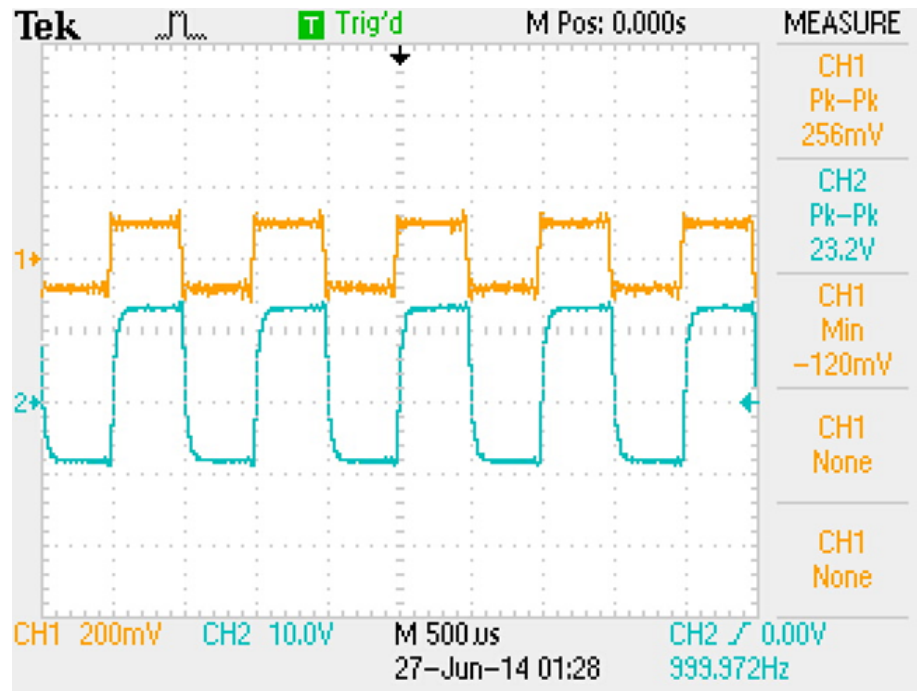


Figure 4.12 Square input signal is at 1000 Hz and 256 mV_{pp} where the output signal is at 1000 Hz and 23.2 V_{pp} .

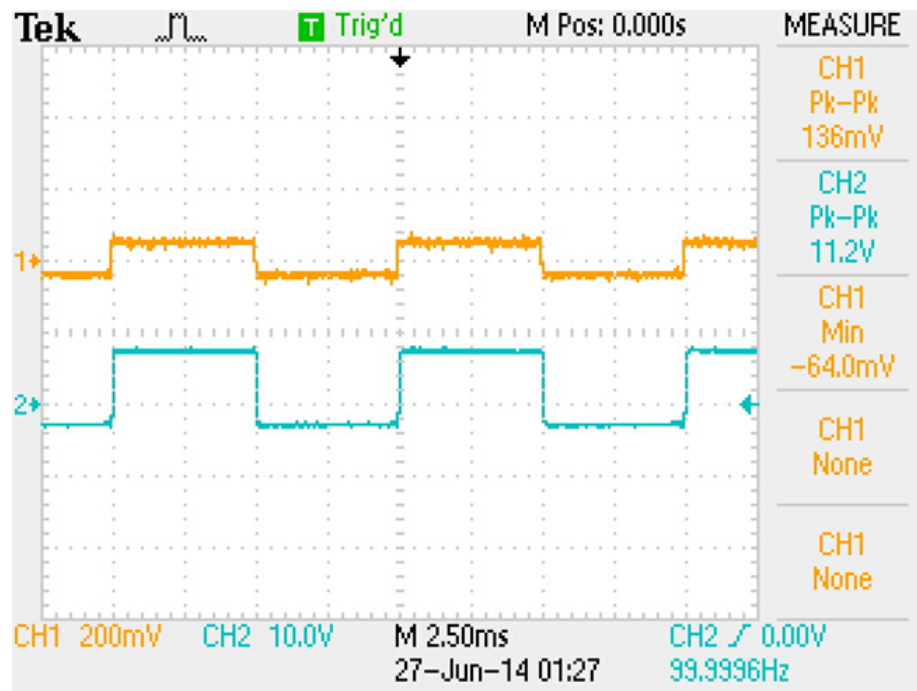


Figure 4.13 Square waveform input signal is at 100 Hz and 136 mV_{pp} where the output signal is at 100 Hz and 11.2 V_{pp} .

Table 4.2

Latency values of previous study of Hayton et al. [14]. Current intensity is $1 - 2 \text{ mA}$ with 3s^{-1} frequency and 0.1 ms duration.

Latency (ms)	
Onset	11.85
P1	15.98
N1	20.53

Table 4.3

Latency values of our physiological experiment.

Experiment conditions	SEP1	SEP2	SEP3
Current intensity (mA)	2	2	10
Duration (μs)	100	100	250
Frequency (pps)	1	1	1
Latency (ms)			
Onset	8	9	9.5
P1	11.8	14	13.5
N1	18.5	21	20

Table 4.4

Amplitude values of previous study of Hayton et al. [14]. Current intensity is $1 - 2 \text{ mA}$ with 3s^{-1} frequency and 0.1 ms duration.

Amplitude (μV)	
Onset to P1	7.25
P1 to N1	8.55

Table 4.5

Amplitude values of physiological experiment.

Experiment conditions	SEP1	SEP2	SEP3
Current intensity (mA)	2	2	10
Duration (μs)	100	100	250
Frequency (<i>pps</i>)	1	1	1
Amplitude (μV)			
Onset to P1	4.8	1.4	1.8
P1 to N1	11.8	3.2	4

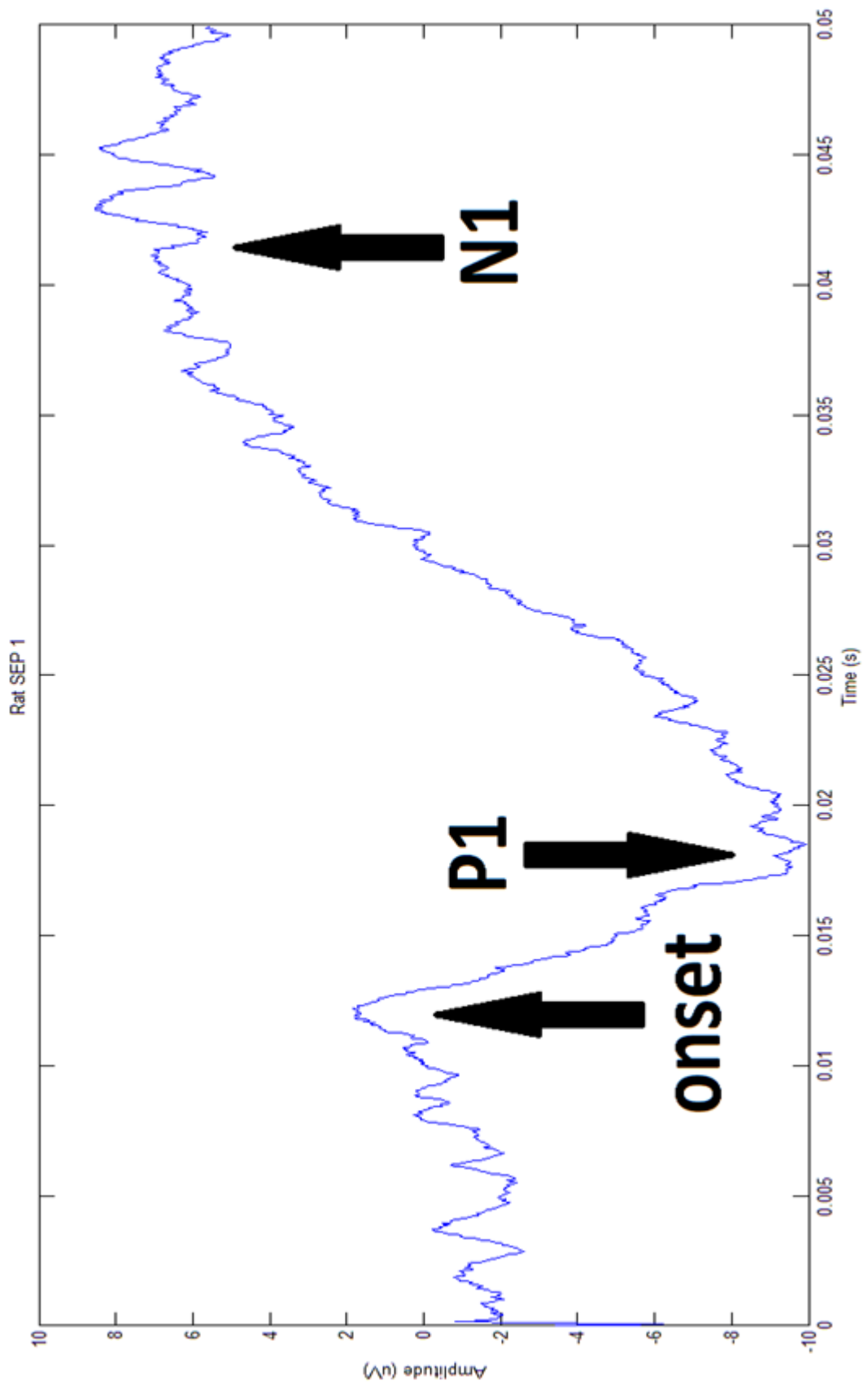


Figure 4.14 Averaged SEPs from rat under anesthesia after first injection, current of 2 mA at a pulse width of 100 μ s and averaged at 100.

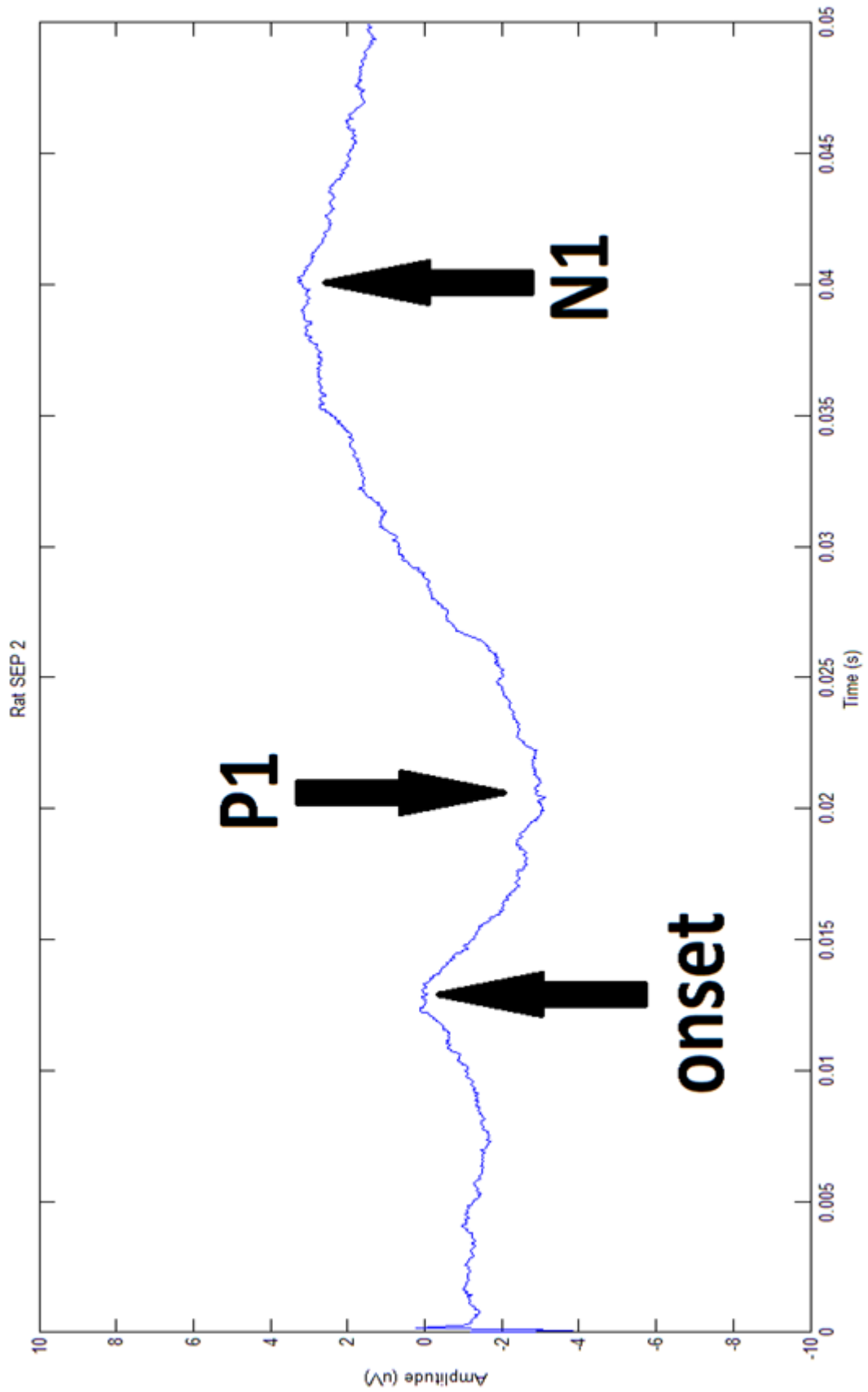


Figure 4.15 Averaged SEPs from rat under anesthesia after second injection, current of 2 mA at pulse width of 100 μ s and averaged is 400.

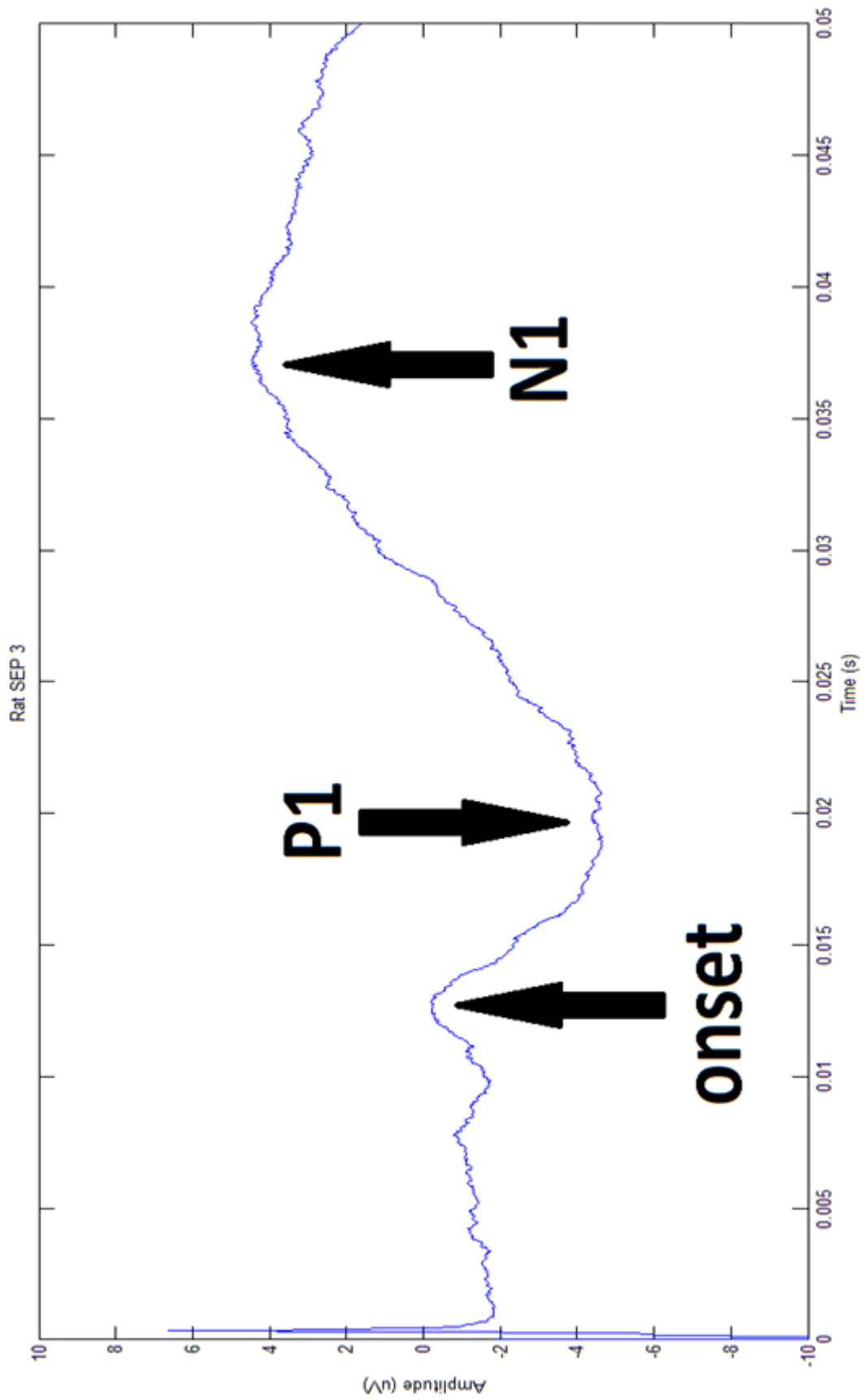


Figure 4.16 Averaged SEPs from rat under anesthesia after second injection, current of 10 mA at pulse width of 250 μ s and averaged is 370.

5. DISCUSSION

The stimulator device has been tested in both electrical and biological experiments. Experiments showed that the device is compatible for laboratory use. The device is simple to build and inexpensive. However, there are some engineering and biological limitations which are discussed below.

5.1 Limitations

5.1.1 Engineering Limitations

The biggest problem with the stimulator is the mismatch in the resistor (Eq. 3.13) because the device handmade the resistors used did not satisfied this relationship exactly. As a result, the current output was not constant for wide range of load resistances. In other word, the output resistance was not very high. However the performance of the device was still acceptable for biological applications in which the electrodes-tissue impedance is not high.

Another important limitation of the stimulator is the limited compliance. During the design, the voltage supply had to be limited according to the maximum rating of the Op amp. This limited the maximum current supplied by the device at high load resistances. Similarly the ratings of the other IC limit the maximum command voltage, and therefore the current output from the device.

For simplicity and reduce costs we use a sound card to generate stimulus waveforms. However the sound card is designed for audio frequencies, therefore it does not output dc voltages this reduced the maximum current pulse width available in our device. The power supply unit is also bulky compared to the commercial stimulator devices.

It was observed that the output of the ISO 124 somewhat is noisy therefore I had to use a RC filter to get rid of high frequency noise. Different types of isolation

units can be used in future design.

5.1.2 Biological Limitations

Since we used needle electrodes, under the skin, the electrode tissue impedance was low compared to other studies. However, the current spread at the tip of the electrode could not be controlled due to the small size of the rat. In order to perform a more controlled experiment the electrode geometry and the location should be precisely determined. Similarly scalp electrodes were placed crudely over the somatosensory cortex. However, I did not use a brain atlas. Therefore the somatosensory evoked potentials measurement was not up to the clinical standards.

The anesthesia level of the animal was not tightly controlled. The animal was lightly sedated and additional doses were given if needed according to reflexes since this was only a demonstration experiment we did not control the vital signs precisely. However, we made sure that the somatosensory evoked potential was measured at a minimum current level which produced a muscle twitch response. This is the standard criteria used clinically. The normal ranges of latencies and peak amplitudes are typically given for awake subjects since it would be very hard to measure SEPs in awake rats we had to anaesthetize the animal. Since the device is not approved for human use we did not test it on humans. However, the results show that it can be used on humans with small modification in the design.

5.2 Comparison with Previous Stimulators

Previous stimulators are made of different topologies. Some of the previous circuits lack the isolation unit or flexibility of control. Some are expensive. Our improved Howland-type electrical stimulator satisfies many requirements listed in the introduction section. The output current is limited due to the op amp itself but applying parallel op amps or using external transistors, the current can be boosted up considerable ($\approx 1 A$) however such high currents are not typically used in biological

applications. For example, the maximum output from FES devices is below 200 mA .

Commercial devices such as Model DS7A by Digitimeter, 6002 Basic Stimulator by Harvard apparatus (\$ 1,400), SD9 Square-Pulse stimulator by Grass Technologies (\$ 1,700), BSL Stimulator by BIOPAC systems (\$ 3,600), Model 2100 Isolated pulse stimulator by A-M system (\$ 1,800) and DS8000 World precision Instruments (\$6,000), are expensive. These devices can be afforded for research purposes. Clinical devices may be even more expensive. However, an inexpensive design as presented in this thesis is more suitable for student laboratory.

During my literature search I also found custom-made stimulators. It is possible to find custom-made stimulator designs for use in different areas such as electrical impedance tomography (EIT), electromyography (EMG), functional electrical stimulation (FES), functional neuromuscular stimulation (FNS) etc. typically, custom-made stimulators are used for specific applications in which commercial devices are not adequate.

In Güçlü's [3] study, which was the basis for my thesis, the range of compliance is $\pm 15 V$ so the maximum current can be 1.5 mA at 10 $k\Omega$ load resistance. The design is very practical for student laboratory experiment on physiology. However, due to the insufficient compliance for transcutaneous stimulation, a power op amp was used in this thesis which allowed higher compliance and higher current output.

The study of Tuckers et al [12]. is on Electrical impedance tomography, and therefore they needed wide frequency range of 1 kHz to 1 MHz where the current is about 2 mA . They designed a constant current source with improved Howland-type design. They obtained a very high output impedance of 3.3 $M\Omega$ because they used resistors with 0.01 % tolerances so eq. 3.13 is satisfied with a better match. On the other hand our resistors are 1 % tolerances, so output impedance could not be as high in our design.

In the McPartland et al. [15] study, current injection ability of their device is 100 mA in a range between 10 – 60 Hz and pulse width is 1000 μs . The stimulators, with higher current injection ability, sometimes cannot act as high precision devices so in SEPs or subdermal applications they cannot be used. This kind of devices cannot produce current at micro ampere levels and the high current values may produce tissue damage if proper electrodes are not used. This device may be used for muscle

stimulations.

In the study of Varghese et al. [24] device is designed to be used as functional neuromuscular stimulation for paralyzed muscles. The output current of device is in the range of $0 - 20 \text{ mA}$ with a resolution of 1 mA . Time period of stimulation is $1 \text{ ms} - 1 \text{ s}$. The pulse duration range is $1 - 250 \text{ ms}$. However, the resolution of the device is not sufficient for microstimulation.

As a summary the stimulator presented in this thesis is not as powerful as FNS. However it has good resolution to be used as direct nerve stimulation in situ and nerve and muscle stimulation transcutaneous.

5.3 Suggestions for Improvement and Future Work

The device may be redesigned by using surface-mount component in order to minimize the size. Toroidal transformers are available for power supply unit. Power supply of the system was huge, therefore more portable power supply is required. A battery can be used instead of a power supply. This provides a better isolation for the system. However, a charging circuit should be added for the battery. Additionally the sound card output should be still isolated by using additional components.

In order to commercialize this design the waveform generation can be achieved by using a microprocessor. The user interface can be improved accordingly by using a touch screen. This kind of improvement will require a considerable effort for development. For research laboratory use it would be adequate to use a data acquisition and control card (for example, National Instruments) instead of the sound card to overcome some of the limitations listed above.

APPENDIX A. Setup Photos

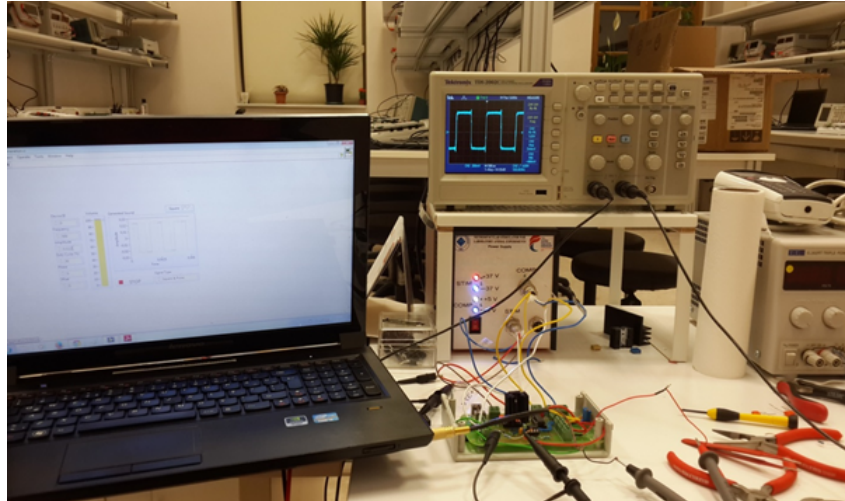


Figure A.1 The stimulator is shown next to the laptop. The power supply is below the oscilloscope.



Figure A.2 The stimulator is shown next to the laptop. The power supply is below the oscilloscope.

REFERENCES

1. Galvani, L., *De viribus electricitatis in motu musculari commentaries*, Northwestern University: Elizabeth Licht, 1953. Bologna University, 1791.
2. DiLorenzo, D. J., and J. D. Bronzino, eds., *Neuroengineering*, CRC Press, 2008.
3. Guclu, B., “Low-cost computer-controlled current stimulator for the student laboratory.,” *advances in physiology education*, Vol. 31, pp. 223–231, 2007.
4. Enderlee, J., S. Blanchard, and J. D. Bronzino, *Introduction to Biomedical Engineering, 2nd Edition*, ELSEVIER Academic Press, 2005.
5. Kandel, E. R., J. H. Schwartz, T. M. Jessell, S. A. Siegelbaum, and A. J. Hudspeth, *Principles of Neural Science, 5th Edition*, McGraw Hill, 2013.
6. Plonsey, R., and R. C. Barr, *Bioelectricity A quantitative approach, 3rd Edition*, Springer, 2007.
7. Purves, D., G. J. Augustine, D. Fitzpatrick, L. C. Katz, A. S. LaMantia, and J. O. McNamara, eds., *Neuroscience, 5th Edition*, Sinauer, 1997.
8. Silbernagl, S., and A. Despopoulos, *Color atlas of physiology, 6th Edition*, Thieme, 2008.
9. <http://www.bioscience.org/2009/v14/af/3431/fulltext.php?bframe=figures.htm> , Download date: 01.07.2014.
10. Grahn, P. J., G. W. Mallory, B. M. Berry, J. T. Hachmann, D. A. Lobel, and J. L. Lujan, “Restoration of motor function following spinal cord injury via optimal control of intraspinal microstimulation: toward a next generation closed-loop neural prosthesis.,” *Front Neurosci.*, Vol. 8, no. 296, pp. 1–12, 2014.
11. Franco, S., *Design with operational amplifiers and analog integrated circuits, 3rd Edition*, McGraw-Hill, 2002.
12. Tucker, A. S., and R. J. S. R. M. Fox, “Biocompatible, high precision, wideband, improved howland current source with lead-lag compensation.,” *Biomedical Circuits and Systems-IEEE*, Vol. 7, pp. 63–70, 2012.
13. Romo, R., A. Hernandez, A. Zainos, and E. Salinas, “Somatosensory discrimination based on cortical microstimulation.,” *Nature*, Vol. 392, pp. 387–390, 1998.
14. Hayton, S. M., A. Kriss, and D. P. R. Muller, “Comparison of the effects of four anaesthetic agents on somatosensory evoked potentials in the rat.,” *Laboratory Animals*, Vol. 33, pp. 243–251, 1999.
15. McPartland, M. D., and D. J. Mook, “A robust transcutaneous electro-muscle stimulator (rtes): a multi-modality tool.,” *Med. Eng. Phys.*, Vol. 17, no. 4, pp. 314–318, 1995.
16. F. S. Jaw and, S. J. L., T. S. Kuo, and C. Y. Wang, “Microcomputer-based pulse stimulator.,” *Journal of Neuroscience Methods*, Vol. 62, pp. 193–197, 1995.
17. Millar, J., T. G. Bamett, and S. J. Trout, “The neurodyne: a simple mains-powered constant-current stimulus isolator.,” *Journal of Neuroscience Methods*, Vol. 55, pp. 53–57, 1994.

18. Misulis, K. E., and T. Fakhoury, *Spehlmann's evoked potential primer, 3rd Edition*, Butterworth Heinemann, 2001.
19. Johnson, C. D., *Process control instrumentation technology, 8th Edition*, Pearson, 2006.
20. Pouliquen, P., J. Vogelstein, and R. Etienne-Cummings, "Practical consideration for the use of a howland current for neuro-stimulation," *Biomedical Circuits and Systems Conference IEEE*, pp. 33–36, 2008.
21. Horowitz, P., and W. Hill, *The Art of Electronics, 2nd Edition*, Cambridge University Press, 1989.
22. Scherz, P., *Practical electronics for inventors*, McGraw-Hill, 2000.
23. Rubinstein, J. T., C. A. Miller, H. Mino, and P. J. Abbas, "Analysis of monophasic and biphasic electrical stimulation of nerve," *Biomedical Engineering, IEEE Transactions*, Vol. 48, no. 10, pp. 1065–1070, 2001.
24. Varghese, B., B. K. Gopal, S. George, and P. K. Joseph, "Low cost general-purpose microcontroller based multi-channel neuromuscular stimulator," *ITBM-RBM*, Vol. 26, pp. 291–295, 2005.